July 5, 2019

Dear Prof. Herckes,

Please find enclosed our response to the reviewers for manuscript amt-2019-45 ("An Extractive Electrospray Ionization Time-of-Flight Mass Spectrometer (EESI-TOF) for online measurement of atmospheric aerosol particles)".
This file contains a point-by-point response to the reviewers, with changes to the text marked in blue. We also include a complete version of the manuscript with all modifications marked in "track changes" mode. Aside from the changes noted in response to the reviewers, the only changes made have been to correct a few minor typos.
Thank you for considering our manuscript for AMT, and we look forward to your response.

Best regards,
Jay Slowik

Response to Reviewer #1

We thank the reviewer for the helpful comments, which have helped improve the manuscript. Below we provide a point-by-point response to the issues raised by the reviewer. Reviewer comments are provided in *italics*, our responses follow in normal text, and modifications to the manuscript are denoted in blue.

Comment #1:

The term "near-molecular level" is used a few times. I assume this refers to MS measuring masses only instead of really individual compounds, but the term should be explained in the paper. A word of caution regarding quantitative results from mass measurements vs. fully resolved (chromatography) measurements might be justified as well.

Response:

As the reviewer surmises, we use the term "near-molecular level" to indicate that the EESI-TOF can provide a molecular formula but no direct structural information or isomeric separation. We have clarified this term "near-molecular level" in two places:

Abstract: "To address this gap, we present a novel, field-deployable extractive electrospray ionization time-of-flight mass spectrometer (EESI-TOF), which provides online, near-molecular (i.e., molecular formula) OA measurements at atmospherically relevant concentrations without analyte fragmentation or decomposition."

Section 2.1: "The EESI source was developed with the specific goal to measure OA at a near-molecular level (with "near-molecular" here defined as the determination of a molecular formula, without direct structural information or isomeric separation), however it can more generally be applied to gas or combined gas/particle measurements."

We also agree with the reviewer's second point, namely that the possibility of isomers can complicate quantification in experimental or field measurements even if the relevant standards are available. This issue was also raised by Reviewer #2 (Comment #17). We have added the following text to section 3.2, where quantification of EESI-TOF data is considered.

"Further, for aerosol of unknown composition the possibility of multiple isomers (potentially having significantly different RRF_x) must be considered."

Comment #2:

P7L7-8: What was the flow rate?

Response:

The flow rate is between 0.7 and 1.0 L min^{-1}, depending on the temperature of the inlet capillary. This information has been added to the manuscript.

Comment #3:

What does "most species" mean? Which species are not removed and could this pose a problem? Related, could 0.x % denuder breakthrough distort results for volatile species with high gas-phase and very low particle phase concentrations?

Response:

Questions related to denuder performance were also raised by Reviewer #2 (Comment #8), and our response is duplicated here.

We agree with the reviewer that denuder breakthrough is problematic, as it can result in either increased detection limits or spurious particle signal. These issues were noted in the original manuscript in section 2.1 as motivation for installing the denuder and we leave the original text

unchanged except that we now note that these problems can arise not only from the absence of a denuder but also from breakthrough.

We have not conducted a comprehensive, compound-by-compound assessment of the denuder. The term "most species" was instead meant to indicate that for the systems discussed in this manuscript (i.e., pure components, laboratory-generated SOA, and initial ambient measurements in Switzerland), breakthrough has not been observed. More recently, we have experienced some breakthrough issues in heavily polluted ambient locations. Characterization of these effects is ongoing and preliminary results suggest this problem can be solved without degrading performance simply by utilizing a larger denuder.

We now discus this in section 2.1 as follows: "The denuder is very similar to that used for the CHARON-PTRMS, where it removes methanol, acetonitrile, acetaldehyde, acetone, isoprene, methylethylketone, benzene, toluene, xylene, 1,3,5-trimethylbenzene, and α-pinene with >99.9999% efficiency (Eichler et al., 2015). Our experiments show >99.95% removal for pinonic acid, and no detectable breakthrough in the chamber and field experiments presented in section 4, which were conducted at OA concentrations up to approximately 10 µg m^{-3} with the denuder not requiring regeneration for at least 2 weeks. For smog chamber experiments on wood and coal-burning emissions at higher concentrations (20 to 200 µg m^{-3}, 1 experiment of 3-4 h per day) (Bertrand et al., submitted), the denuder was regenerated every 2 to 3 days, when a slower response time was observed on switching between the direct sampling and filter blank measurements. This suggests a higher capacity denuder should be used for continuous sampling under polluted conditions."

Comment #4:

P9-10: I appreciate the discussion on pros and cons of different ESI mixtures, but was a bit surprised to read that MeOH/H2O was used at the end for most studies. My impression from the discussion was that overall ACN/H2O might be more suitable, especially due to the stated high background peaks in MeOH/H2O. Please comment on this final choice.

Response:

The main consideration is that operationally the MeOH/H2O spray is easier to stabilize and so was chosen for both the initial characterization experiments presented here and early measurement campaigns (Pospisilova, Stefenelli). With improved machining of the EESI source and increased user experience, the ACN/H2O mixture has become our preferred working solution for most applications (e.g., Qi) because of its lower background, as correctly identified by the reviewer. As a consequence, the set of characterization experiments performed for the MeOH/H2O system is presently more comprehensive than that of the ACN/H2O system, and we therefore choose to focus on MeOH/H2O results here while noting their comparability to ACN/H2O, rather than the reverse.

Comment #5:

P13L1-6: Is the usage of mass flux for some and ion flux for most other results really justified? It adds some complexity and the advantage of using mass flux in ag/s is not fully clear to me.

Response:

This issue was also raised by Reviewer #2 (Comment #2), and our response is repeated here.

Most studies describe particle-phase composition in terms of mass. Therefore, when discussing total EESI-TOF signal or relative composition, we utilize the mass flux metric. This is the quantity most closely related to mass that we can obtain given the unknown RRF_x.

However, a large part of this paper also focuses on the fundamental operation of the EESI-TOF. Here it is desirable to present results in terms of the actual quantity measured (i.e., ion flux), which in our view makes instrument operation/response most transparent. For example, although ionization efficiency and related concepts (Eq. 1 and related discussion), as well as the RRF_x, can be in principle discussed in terms of mass, these concepts and the obtained values are most clear when presented in terms of the probabilistic behavior of individual ions and molecules.

We have clarified this in the manuscript as follows (section 3.1):

"Fundamentally, the EESI-TOF measurement is in terms of the ion flux reaching the detector (Hz), as shown on the left axis of Fig. 2. However, in most studies the particle phase is described in terms of mass for both absolute and relative concentrations, making it desirable to also obtain a mass-related metric from the EESI-TOF measurements. In principle, the EESI-TOF ion signal for a molecule *x* can be converted to a mass concentration according to Eq. (1):"

"For reference, we show on the right axis of Fig. 3 the MF_x (in attograms (10^{-18} g) per second, ag s^{-1}) corresponding to the measured I_x; however for the remainder of the basic characterization experiments presented herein we show instead the directly measured I_x, which is the actual quantity measured by the instrument."

Comment #6:

P14L30 + abstract + conclusions: I find the statement of the "much smaller range" the RRFx spans for SOA as compared to pure components a bit misleading. Given it represents a mean value for a very complex mixture, it is not surprising it varies less than individual compounds. Even more, with Benzene included (its exclusion seems quite arbitrary), the difference to the studied pure model compounds becomes smaller.

Response:

This issue was also raised by Reviewer #1 (Comment #6) and our response is duplicated here.

In the original manuscript, benzene was classified empirically as an outlier because its removal has a considerably larger effect on the range of SOA RRFs (60 % decrease) than does removal of either the highest RRF (1,3,5-trimethylbenzene, 40 % decrease) or the next lowest (phenol, 30 %). However, the low RRF observed for benzene is consistent with the overall observed trend, and we therefore agree it can be misleading to treat it separately. The revised text simply notes that the range of RRFs observed for SOA is lower than that for the pure compounds, while noting that the pure compounds must occupy a larger range than indicated because the RRF for benzene SOA is

a factor of 3 lower than any of the pure components. As noted by Reviewer #1, this decreased RRF range for SOA is expected given that it represents the mean RRF of a complex mixture.

The revised text is as follows. "The RRF_x observed for the SOAs span a much smaller range than do the pure components, i.e. a factor 15 between benzene and 1,3,5-trimethylbenzene compared to a factor of ~30 between citric acid and dipentaerythritol (note that the range of RRF_x for pure components is an underestimate, as some pure components must have an *RRF* at least as low as benzene, which is itself a factor of 3 lower than citric acid). The smaller RRF_x range exhibited by the SOA experiments is expected given that each value represents the mean *RRF* of a complex mixture and is consistent with ambient observations, where we do not observe major composition-dependent variations in overall EESI-TOF sensitivity to bulk ambient OA (Qi et al., 2019; Stefenelli et al., 2019). However, direct calibration is clearly advisable for compounds for which absolute quantification is desired. Further, for aerosol of unknown composition the possibility of multiple isomers (potentially having significantly different RRF_x) must be considered."

The corresponding text in the abstract and conclusions has also been modified.

Abstract: "Although the relative sensitivities to a variety of commercially available organic standards vary by more than a factor of 30, the bulk sensitivity to SOA generated from individual precursor gases varies by only a factor of 15."

Conclusions: "The EESI-TOF sensitivity to SOA generated from a set of individual precursor gases varies within a factor of 15."

Comment #7:

P17L3-4 + abstract + conclusions: The conclusion on the absence of matrix effects seems to be based on dipentaerythritol experiments only. The insensitivity of this single compound to the specific particle matrix studied cannot, however, be generalized. From conventional ESI it is well known that some species are more susceptible to matrix effects than others. In addition, the organic matrix in these experiments is certainly not representative to the full range of real world particle matrices (both organic and inorganic). I would recommend more caution here. A general absence of any particle matrix effects can only be demonstrated by detailed comparisons with GC/LC-MS based quantification.

Response:

We agree that the presence and extent of matrix effects may depend on the identity of the test compound and/or the surrounding matrix. A single case study (dipenaerythritol in SOA α-pinene ozonolysis) is presented in this manuscript; investigation of a large number of systems is beyond the scope of the current work. However, we have also compared the total EESI-TOF OA signal to the detectable fraction of AMS OA (i.e., SOA and oxygenated POA) for ambient aerosol (Qi et al., 2019; Stefenelli et al., 2019), as well as laboratory-generated aerosol that is internally mixed with $(NH_4)_2SO_4$ and/or NH_4NO_3. In general, good agreement was observed and discrepancies were explainable by the expected differences in RRF_x. Although encouraging, this does not altogether rule out matrix effects for individual OA ions. However, it does indicate that bulk OA sensitivity is likely unaffected by a soluble inorganic matrix.

The following text has been added to section 3.3:

"Although these results are obtained from a single test system, they are consistent with the general trend of matrix effects in EESI studies that are negligible or strongly suppressed relative to conventional electrospray measurements (Chen et al., 2006; Gu et al., 2007; Zhou et al., 2007; Chen et al., 2009). In addition, we find that OA signals measured by the EESI-TOF are well correlated with AMS measurements (e.g. total measurable OA, source apportionment factors, tracer ions) (Qi et al., 2019; Stefenelli et al., 2019). This suggests that EESI-TOF bulk OA measurements are likely not affected by soluble inorganic matrices typical of Central Europe (i.e., internal mixtures with NH_4NO_3 and $(NH_4)_2SO_4$ concentrations up to ~10 µg m^{-3}), although effects on individual ions cannot be ruled out."

We have also qualified statements in the abstract and conclusions, as follows:

Abstract: "In contrast to conventional electrospray systems, the EESI-TOF response is not significantly affected by a changing OA matrix for the systems investigated."

Conclusions: "We observe an instrument response that is linear with mass and without a detectable dependence on the composition of the OA matrix for a dipentaerythritol/α-pinene SOA test system. Ambient measurements also suggest that bulk OA detection is not significantly affected by a changing matrix of soluble inorganic compounds."

Comment #8:

P18L2-5: Can you comment on possible mechanisms of water vapor interference?

Response:

The following text has been added to section 3.4: "Water can potentially decrease sensitivity by competing with the analyte for Na^+ ions (e.g. by displacing the analyte), or increase sensitivity by absorbing energy from Na^+-adducts, thereby stabilizing them."

Response to Reviewer #2:

We thank the reviewer for the thoughtful and detailed review, which has allowed us to improve the manuscript. Below we provide a point-by-point response to the issues raised by the reviewer. Reviewer comments are provided in *italics*, our responses follow in normal text, and modifications to the manuscript are denoted in blue.

Comment #1:

Improved detection limits (DL) is noted throughout the manuscript as a major advance (if not the main one) for this new instrument configuration. However, only a couple general statements are provided regarding DLs (e.g., p13 ln 18-21) without sufficient details to fully understand this key aspect (see additional comment below). I would have expected a subsection in section 3 to be dedicated to showing DLs for a range of elemental formulae or compounds such as those shown in some of the dense example spectra. Also, dependency on sampling time or sampling history, solvent type, compound or m/z and other important aspects that may affect DLs as would be typical

in an instrumental characterization paper like this one. Perhaps a mass spectrum of DLs would be appropriate (probably requiring assignment of an approximate fixed sensitivity).

Response:

This is an excellent idea. We now present approximate detection limits determined from the summer field campaign in Zurich in section 4.2. Figure 10 has been modified accordingly. Figure 10a consists of the original Fig. 10 (campaign average mass spectrum, colored by ion type). We have added Fig. 10b, which shows detection limits (30 s) calculated as 3-σ variation of the respective ion signal during the filter blank, and assuming a sensitivity of 1450 cps per μg m^{-3}, corresponding to the estimated bulk sensitivity for SOA during this campaign (Stefenelli et al., 2019). The same color scale is used as in Fig. 10a. Figure 10c shows the results from Fig. 10b in histogram form.

The following discussion addressing the revised Fig. 10 has been added to the manuscript: "Estimated detection limits (30 s) are shown on an ion-by-ion basis in Fig. 10b, using the same color scheme as in Fig. 10a. Detection limits are calculated as the 3-σ variation of the ion signal during the filter blank periods flanking a direct sampling interval, and the campaign median is shown. Detection limits are converted to mass assuming a uniform sensitivity of 1450 Hz / (μg m^{-3}), which corresponds to the estimated sensitivity of SOA during this campaign (Stefenelli et al., 2019). This is a rough estimate which neglects ion-dependent sensitivities and differences in molecular weight. The results are summarized in histogram form in Fig. 10c. Most species have detection limits in the range 1 to 10 ng m^{-3} (median 5.4 ng m^{-3}), with nitrogen-containing ions having slightly lower detection limits than other species. We note that these measurements utilized a methanol:H_2O working solution, and detection limits from the cleaner acetonitrile:H_2O system will likely be lower."

Comment #2:

Both mass flux and Hz are used throughout the plots in the paper for signal metrics in various places. Can the authors explain this choice (using one vs. the other)? Is it preferred to reflect the mass weighting of the ion signals when showing multiple compounds such as the mass spectra, while not needed for showing single ions? Or if there is not uniform reasoning behind this, perhaps consider using a consistent metric throughout?

Response:

This issue was also raised by Reviewer #1 (Comment #5), and our response is repeated here.

Most studies describe particle-phase composition in terms of mass. Therefore, when discussing total EESI-TOF signal or relative composition, we utilize the mass flux metric. This is the quantity most closely related to mass that we can obtain given the unknown RRF_x.

However, a large part of this paper also focuses on the fundamental operation of the EESI-TOF. Here it is desirable to present results in terms of the actual quantity measured (i.e., ion flux), which in our view makes instrument operation/response most transparent. For example, although

ionization efficiency and related concepts (Eq. 1 and related discussion), as well as the RRF_x, can be in principle discussed in terms of mass, these concepts and the obtained values are most clear when presented in terms of the probabilistic behavior of individual ions and molecules.

We have clarified this in the manuscript as follows (section 3.1):

"Fundamentally, the EESI-TOF measurement is in terms of the ion flux reaching the detector (Hz), as shown on the left axis of Fig. 2. However, in most studies the particle phase is described in terms of mass for both absolute and relative concentrations, making it desirable to also obtain a mass-related metric from the EESI-TOF measurements. In principle, the EESI-TOF ion signal for a molecule *x* can be converted to a mass concentration according to Eq. (1):"

"For reference, we show on the right axis of Fig. 3 the MF_x (in attograms (10^{-18} g) per second, ag s^{-1}) corresponding to the measured I_x; however for the remainder of the basic characterization experiments presented herein we show instead the directly measured I_x, which is the actual quantity measured by the instrument."

Comment #3:

Title: the title refers to the EESI-TOF instrument, but the paper is all about the EESI source with no new information or modification for the TOF mass spectrometer. A TOF does not seem strictly needed either, and EEIS has been used before with other mass analyzers. I strongly suggest that the title is updated to reflect this, to something like "An extractive electrospray (EESI) ion source for online mass spectrometric measurements…"

Response:

The motivation for the development of this instrument is to fill an important gap in existing OA measurements, namely an online, highly time-resolved, field-deployable system with a relatively controlled ionization scheme and sufficient detection limits for ambient operation, but without analyte decomposition or fragmentation. We achieved this through the development of a new EESI source, optimized for and coupled to a specific TOF-MS. Although we agree that, in principle, the EESI source presented here can be adapted to other mass spectrometers, it is not clear that all of these capabilities will be preserved. As a simple example, the ion transmission efficiency of the specific TOF-MS used here is an important factor in achieving the requisite detection limits. Likewise, the specific construction of the TOF-MS capillary inlet limits the range of accessible temperatures and time spent at/near atmospheric pressure post-extraction.

As a result, we strongly feel that adaptation of this EESI inlet to a new instrument creates a system which once again requires fundamental and comprehensive characterization, and is thus best considered a separate instrument. To avoid confusion on this point, we therefore prefer to retain the original manuscript title.

We now note this instrument vs. source issue in sensitivity discussion in Section 3.2: "Note that these improved detection limits represent the performance of the entire EESI-TOF instrument relative to previous instruments, and we cannot disentangle the contributions of the ionization unit and MS detector."

Comment #4:

P1 ln 13: DLs without the relevant sampling time are meaningless, please state.

Response:

The revised text reads: "The EESI-TOF achieves a linear response to mass, with detection limits on the order of 1 to 10 ng m^{-3} in 5 s for typical atmospherically-relevant compounds."

Comment #5:

P6 ln 3-7: Again, it is unclear what the relevant sampling period for the stated numbers are, please clarify. Strictly speaking, the amount of sample should be stated as well, but given the similarity of the discussed instruments they are probably comparable.

Response:

We agree that this information would be useful, however it is not available from the cited literature. We are able to provide integration times for the Gallimore et al. system, however: "A more recent EESI system (Gallimore and Kalberer, 2013; Gallimore et al., 2017) attained individual compound detection limits of ~1 µg m^{-3} for 100 s integration (M. Kalberer, private communication), which were further reduced to as low as 0.25 µg m^{-3} using tandem mass spectrometry (MS^2) and collisionally-induced dissociation (CID)."

Comment #6:

P6 ln 11-14: This statement about "EESI" is unclear whether it refers to previous work or this paper. Probably previous work since it comes before the final paragraph stating what is presented in this paper? If so, provide references?

Response:

This refers to the Gallimore and Kalberer (2013) study discussed earlier in the paragraph. The reference is now repeated for clarity.

Comment #7:

P7 ln 4-5: It is stated that 1 um Teflon filters are used for blanks. Often for online aerosol instruments, hepa filters with small pressure drops under extended aerosol exposure are used for blanking. Can the authors comment on any issues with pressure differences associated with switching between filter/no-filter during extended sampling with a clean filter and as the filter loads up with aerosol since substantial pressure changes (~20 mbar) might substantially alter the spray. It is noted later (P12 ln 2-3) that only a 2% change in the [NaI]Na^+ ion was observed during filter switching during sampling of ~30 ug/m3 of a-pinene ozonolysis SOA, however from that it is not clear how well this type of filtering works under extended operation of polluted air. Did the authors operate with this type of filter for the proof-of-concept tests described in Section 4? It would also seem that using a Teflon, low surface area, filter could have less potential artifacts from adsorption/desorption of sticky gases, than HEPA filters with large surface areas

composed of glass or plastics. Thus, providing more information/experience on this aspect could be of substantial value for future users of this source.

Response:

The 1 µm Teflon filters were used for the laboratory characterization experiments. The measurements described in section 4 instead used a nylon cartridge filter (Parker Balston, 9933-11-BQ), which is now noted in the manuscript. These two options provided very similar performance. A HEPA filter was tested in one very recent campaign, but evaluation of its performance is ongoing. Regardless of filter type, we expect that some amount of absorption/desorption is inevitable, however these artifacts are removed by a properly functioning denuder.

The magnitude of the change in the $[NaI]Na^+$ signal depends primarily on the details of spray optimization. Thereafter, during stable operation (i.e. without clogging or user adjustments) we have not observed this value to change in response to increased filter loading. However, during high concentration studies the filter is changed regularly to minimize challenge to the denuder by desorbing semivolatile material, and this maintenance schedule may also prevent us from observing the suggested effect.

The following text has been added to the manuscript: "For the proof-of-concept deployments discussed in Section 4, this filter was replaced with a nylon cartridge filter (9933-11-NQ, Parker Balston, Lancaster, NY, USA), which performed similarly."

Comment #8:

P7 ln 7: the gas-phase denuder seems quite small for this application. What is its capacity? Has breakthrough been tested? How often does it need to be replaced, as a function of sampled concentration?

Response:

Questions related to denuder performance were also raised by Reviewer #1 (Comment #3), and our response is duplicated here.

We agree with the reviewer that denuder breakthrough is problematic, as it can result in either increased detection limits or spurious particle signal. These issues were noted in the original manuscript in section 2.1 as motivation for installing the denuder and we leave the original text unchanged except that we now note that these problems can arise not only from the absence of a denuder but also from breakthrough.

We have not conducted a comprehensive, compound-by-compound assessment of the denuder. The term "most species" was instead meant to indicate that for the systems discussed in this manuscript (i.e., pure components, laboratory-generated SOA, and initial ambient measurements in Switzerland), breakthrough has not been observed. More recently, we have experienced some breakthrough issues in heavily polluted ambient locations. Characterization of these effects is ongoing and preliminary results suggest this problem can be solved without degrading performance simply by utilizing a larger denuder.

We now discus this in section 2.1 as follows: "The denuder is very similar to that used for the CHARON-PTRMS, where it removes methanol, acetonitrile, acetaldehyde, acetone, isoprene, methylethylketone, benzene, toluene, xylene, 1,3,5-trimethylbenzene, and α-pinene with >99.9999% efficiency (Eichler et al., 2015). Our experiments show >99.95% removal for pinonic acid, and no detectable breakthrough in the chamber and field experiments presented in section 4, which were conducted at OA concentrations up to approximately 10 µg m^{-3} with the denuder not requiring regeneration for at least 2 weeks. For smog chamber experiments on wood and coal-burning emissions at higher concentrations (20 to 200 µg m^{-3}, 1 experiment of 3-4 h per day) (Bertrand et al., submitted), the denuder was regenerated every 2 to 3 days, when a slower response time was observed on switching between the direct sampling and filter blank measurements. This suggests a higher capacity denuder should be used for continuous sampling under polluted conditions."

Comment #9:

P7 ln 18: "We find that maximum ion transmission is achieved by maximizing the flow rate into the mass spectrometer, which for our pumping configuration is nominally 1 L min-1". It is unclear to me if the authors are simply stating here that sensitivity simply increases with an increasing ion flux to the mass spectrometer, or if there is an additional benefit of the higher flow. I would also be curious to what extent this effect can be separated from the evaporation process changing with flow, and if this was characterized as part of this work.

Response:

We have empirically observed that the increased ion transmission at high flow rate is greater than can be explained solely by an increase proportional to flow rate. However, this is at present purely an empirical observation, and we are unable to provide further insight into the mechanism.

Comment #10:

P8 ln 6: This statement is too vague. Please provide more information about the estimated temperature or range of temperatures, and the method of estimation.

Response:

Unfortunately, we are unable to be more precise here because we lack the capability to either measure the gas temperature at the capillary outlet or to model heat transfer throughout the entire inlet system. Although admittedly less informative than we would like, we do consider the current statement accurate given the short residence time and the fact that the 240 °C temperature is measured at the heating unit rather than the actual capillary walls. This latter point was not in the original manuscript, but has been added.

Comment #11:

P8 ln 19: is this 1 L min-1 STP, or at some reduced pressure going into the MS?

Response:

We have clarified that this flow rate is at STP.

Comment #12:

P10 ln 15: how was this binding energy quantified?

Response:

We apologize for omitting the references (Rodgers and Armentrout, 1999; Pejov, 2002), which in turn rely on a combination of quantum chemical calculations and collision-induced dissociation experiments.

Comment #13:

P 12, ln 24: "In the absence of fragmentation or decomposition, which has not been observed for any system presented herein". It is unclear how the authors reach this conclusion, it is not supported by the data presented. While it is indeed encouraging that the pure compounds measured by the EESI-TOF in this manuscript did not decompose during analysis (although none of them are particularly unstable), this certainly cannot be shown for the various types of SOA analyzed, since its composition is not known otherwise. The similarity of the EESI and FIGAERO results, which are known to be affected by decomposition (Lopez-Hilfiker et al., 2016, cited in the manuscript, also Stark et al., ES&T 2017), suggest that the EESI might also have some degree of decomposition or fragmentation.

More importantly, this study does not present any indirect evidence that the chemical compositions identified by EESI are indeed consistent with no fragmentation. E.g. in the CHARON instrumental manuscript (Mueller et al., 2017) a comparison of O:C ratios for bulk (AMS) and CHARON was performed, showing – as expected – a lower O:C in the CHARON consistent with some fragmentation/elimination of oxygenated fragments. Such a comparison for the EESI-TOF for one of the simpler SOA cases would increase confidence that the effects of decomposition and fragmentation are low. In the absence of such supporting evidence, I would strongly qualify the above statement.

Response:

We agree that the text highlighted by the reviewer gives the impression that we have performed a detailed assessment of thermal decomposition for every aerosol measured in the paper, which overstates the extent of characterization. The revised text, which is concerned primarily with quantification of individual ions, simply begins: "Assuming no fragmentation or decomposition".

In response to the larger point raised by the reviewer, we provide here some additional information relevant to the understanding of possible thermal decomposition in the EESI-TOF. As noted by the reviewer, we can verify that the pure compounds tested herein did not decompose. This rules out decomposition of aerosol less thermally stable than citric acid (which decomposes at approximately 200 °C).

We agree with the reviewer regarding the difficulty associated with verifying a lack of thermal decomposition in complex aerosol. One way to address this is to ramp the temperature of the capillary. However, as decreasing the capillary temperature increases the instrument gas load, an operational limit is reached when the temperature of the cartridge heaters remain well above room

temperature. Our ability to test hotter temperatures is also limited by hardware constraints on heater operation. Nonetheless, over the range of accessible temperatures, we have observed an increase in sensitivity to α-pinene SOA across the entire mass spectrum with increasing temperature. In the event of thermal decomposition, a decrease in apparent sensitivity would be expected, whereas the increased sensitivity is likely due to more droplet evaporation. Although we cannot rule out the possibility that thermal decomposition occurs at levels small relative to the sensitivity increase, these results do suggest that it is at most a minor effect.

The reviewer also raises comparisons of the EESI-TOF and FIGAERO operation, as potential comparisons between EESI-TOF and AMS atomic ratios. Regarding the EESI-TOF vs. FIGAERO, we note that although the unit temperatures in question are relatively similar, exposure to these temperatures in the EESI-TOF is on the order of 10^5-10^6 times shorter in the EESI-TOF, greatly reducing heat transfer.

Comparison of the atomic O:C ratios between EESI-TOF and AMS have been performed for summer and winter campaigns in Zurich (Qi et al., 2019; Stefenelli et al., 2019). In all cases the EESI-TOF values are greater than or equal to the AMS. However, while ion-molecule reaction rates and thus compound-dependent response factors are well-constrained in the CHARON-PTR system, compound-dependent EESI-TOF extraction efficiencies and RRF_x have not been characterized in detail and may strongly affect the comparison. Therefore we do not believe this data can be used to check for thermal decomposition in the EESI-TOF.

Comment #14:

P13 ln 20-21: Detection limits need associated averaging time information to be meaningful. ~5s, like in Fig. 2?

Response:

Yes, this refers to 5 s measurements (added to the manuscript). Note, however, that we state that 10 ng m^{-3} are "readily detectable" with 5 s of averaging, not that the 5 s detection limits are 10 ng m^{-3} (they are lower).

Comment #15:

P 13 ln 21-23: Are these comparisons of detection limits for other instruments for similar averaging time?

Response:

See response to Comment #5. Averaging times are not reported in the cited manuscripts, although we are able to provide them for the Gallimore et al. system. However, based on the sample data provided in these studies, the times for the other instruments are likely equal or longer.

Comment #16:

P 14 ln 29: The authors describe the EESI-TOF sensitivity to benzene SOA as an outlier compared to the other five SOA systems studied. Looking at Fig. 4 the benzene SOA sensitivity is within the variability of EESI-TOF citric acid sensitivity, and the factor of ~20 difference in bulk SOA

sensitivity (RRFs 0.05 to 1) is similar to the factor of ~30 spread observed for single compounds. There is also a consistent trend in EESI-TOF sensitivity of SOA produced from the homologous series of benzene, toluene, and trimethylbenzene. Additional clarification is needed to justify considering benzene SOA an outlier and excluding it from the calculation of the variability in EESI-TOF SOA sensitivity.

Response:

This issue was also raised by Reviewer #1 (Comment #6) and our reponse is duplicated here.

In the original manuscript, benzene was classified empirically as an outlier because its removal has a considerably larger effect on the range of SOA RRFs (60 % decrease) than does removal of either the highest RRF (1,3,5-trimethylbenzene, 40 % decrease) or the next lowest (phenol, 30 %). However, the low RRF observed for benzene is consistent with the overall observed trend, and we therefore agree it can be misleading to treat it separately. The revised text simply notes that the range of RRFs observed for SOA is lower than that for the pure compounds, while noting that the pure compounds must occupy a larger range than indicated because the RRF for benzene SOA is a factor of 3 lower than any of the pure components. As noted by Reviewer #1, this decreased RRF range for SOA is expected given that it represents the mean RRF of a complex mixture.

The revised text is as follows. "The RRF_x observed for the SOAs span a much smaller range than do the pure components, i.e. a factor 15 between benzene and 1,3,5-trimethylbenzene compared to a factor of ~30 between citric acid and dipentaerythritol (note that the range of RRF_x for pure components is an underestimate, as some pure components must have an *RRF* at least as low as benzene, which is itself a factor of 3 lower than citric acid). The smaller RRF_x range exhibited by the SOA experiments is expected given that each value represents the mean *RRF* of a complex mixture and is consistent with ambient observations, where we do not observe major composition-dependent variations in overall EESI-TOF sensitivity to bulk ambient OA (Qi et al., 2019; Stefenelli et al., 2019). However, direct calibration is clearly advisable for compounds for which absolute quantification is desired. Further, for aerosol of unknown composition the possibility of multiple isomers (potentially having significantly different RRF_x) must be considered."

The corresponding text in the abstract and conclusions has also been modified.

Abstract: "Although the relative sensitivities to a variety of commercially available organic standards vary by more than a factor of 30, the bulk sensitivity to SOA generated from individual precursor gases varies by only a factor of 15."

Conclusions: "The EESI-TOF sensitivity to SOA generated from a set of individual precursor gases varies within a factor of 15."

Comment #17:

P15 ln 8-10: Molecular identification would clearly be a major difficulty in doing this as well. I.e., even if you could just order any compound you wanted, it would be difficult to determine if the isomer detected was the one calibrated for.

Response:

We agree, and have added the following text:
"Further, for aerosol of unknown composition the possibility of multiple isomers (potentially having significantly different RRF_x) must be considered."

Comment #18:
P15/L15 – P16/L9: This section on comparison of EESI-TOF vs. FIGAERO/I-CIMS raw signal seems a bit underdeveloped and potentially susceptible to misinterpretations. The Hz signals of many compounds are compared between the two instruments which show good correlations overall and among ions on a log-log basis. It is stated that I-CIMS reaction rates are collision-limited which in conjunction with adduct binding energies dictate sensitivity, which can be operationally estimated by exploring declustering potential (a.k.a. voltage scanning). Based on the good agreement, it is concluded that therefore the EESI-TOF spectra likely reflect the actual distribution of compounds in particles. However, it has been shown that the relative sensitivities for I- can vary widely; therefore there seems to be a large unsubstantiated logical leap here. I worry that readers will interpret the statement that I-CIMS is collision-limited and seemingly glossed over additional factors controlling sensitivity as meaning that the uncalibrated I-CIMS spectrum essentially reflects the relative distributions of compounds in particles.
Why wasn't the voltage scanning sensitivity estimation method used here? This could help close this gap, providing a more direct look at response factor variability for the EESI for a wide range of atmospheric SOA surrogate compounds? It is especially surprising that this step wasn't taken, given the authors' development of that method. Without calibration or knowing the general instrument sensitivity and declustering settings, it would seem that the slopes don't have much meaning. That said, the good correlation certainly is interesting, useful and promising that the current analysis suggests that empirical sensitivities may be derivable/parameterized for the EESI-TOF.
Response:
We agree with the reviewer that a detailed comparison of the EESI-TOF with the FIGAERO-I-CIMS (or other related instruments) is of high interest, and regarding the potential utility of the voltage scanning for sensitivity estimation. However, these investigations are very complex, whereas the measurements performed for this comparison were intended only as a basic proof-of-principle test with the specific goal of demonstrating that the EESI-TOF response is qualitatively similar to a gas-phase CIMS despite the additional complications of condensed-phase extraction and droplet evaporation/ionization. Because of this limited goal, we did not conduct the voltage scanning suggested by the reviewer and a relatively limited amount of data is available. We have since conducted several dedicated campaigns focused on the inter-comparison of EESI-TOF with related instruments, and prefer to defer a detailed discussion of such inter-comparisons to the presentation of these studies.
The reviewer also identifies the final sentence in section 3.2 ("Further, the correlation [between FIGAERO and EESI-TOF] indicates that the spectral patterns observed in the EESI-TOF likely reflect to a large degree the actual distribution of compounds in the particle phase" as prone to

misinterpretation. We agree, and have removed this sentence. Note also that a detailed discussion of the factors governing I-CIMS sensitivity was presented in the preceding paragraph in the original manuscript.

Comment #19:

P15 ln 23: How representative are the 12 m/z's presented in Fig. 5 of the 100+ shown for the same chemical system in Fig. 9? Namely what fraction of the aerosol signal is attributable to these twelve m/z's? Was the FIGAERO comparison extended to other m/z's?

Response:

The ion series selected for comparison ($C_9H_{14}O_x$ and $C_{10}H_{16}O_x$) together comprise 21% of the EESI-TOF signal and 19% of the particle-phase FIGAERO-I-CIMS signal. This information has been added to section 3.2. As noted in the previous response, the FIGAERO/EESI-TOF comparison was intended only as a basic proof-of-principle test, and we prefer to defer detailed comparisons of the mass spectra to the dedicated inter-comparison campaigns that have since been conducted.

Comment #20:

P16, L27-28: How is this known? Analysis of SMPS distributions? Is the 20 nm seed particle mode separable from the a-pinene ozonolysis nucleation mode? Ensuring that a substantial fraction of the seed is coated seems pretty important to this demonstration. If this is problematic, and nucleation was unavoidable, why weren't larger seed particles used? 20 nm (and growing to 70 nm) seems surprisingly small for this test (and not representative of the size of particles in the atmosphere where most of the mass resides).

Response:

The fraction of coated particles was determined from analysis of the SMPS distributions; this information has been added to the manuscript.

Regarding the selected seed particle size, this reflects the mode of the number distribution generated from our nebulizer. While larger particles would be indeed be desirable to better represent the atmospheric mass mode, we have observed that size-selecting particles with a DMA greatly reduces their detection efficiency by the EESI-TOF (even after passing through a second nebulizer). The reasons for this are not yet clear, but prevented us from attempting the suggested experiments.

We additionally note that good agreement between the total EESI-TOF signal and the relevant fraction of AMS OA (SOA and oxygenated POA) have been obtained for a variety of systems, including ambient accumulation mode particles. This information was added to section 3.3 as follows: "In addition, we find that OA signals measured by the EESI-TOF are well correlated with AMS measurements (e.g. total measurable OA, source apportionment factors, tracer ions) (Qi et al., 2019; Stefenelli et al., 2019). This suggests that EESI-TOF bulk OA measurements are likely not affected by soluble inorganic matrices typical of Central Europe (i.e., internal mixtures with

NH_4NO_3 and $(NH_4)_2SO_4$ concentrations up to ~10 µg m^{-3}), although effects on individual ions cannot be ruled out."

Comment #21:

P17 Section 3.4 (Water vapor dependence): This is a nice analysis. Have the authors considered whether some of the compounds with substantial H2O-dependence effects may be dominated by semi-volatile gases breaking through the denuder? Possibly looking at the humidity-dependence of signals that are enhanced during the filter blanks would help understand that possibility.

Response:

In these experiments, we have not identified any signal attributable to denuder breakthrough (aside from water clusters with ions derived from the working solution or NaI dopant, which are not relevant to the question posed).

Comment #22:

P17 ln 19: it would be informative if the authors reported the relative mass fluxes of water from the ESI and from the sample flow (at let's say 50% RH).

Response:

We assume a sample flow rate of 0.8 L min^{-1} at 25 °C, corresponding to a molecular flux of 2.27 x 10^{20} molec min^{-1} of H_2O. We do not directly measure the flowrate through the ESI capillary, but this is estimated to be in the range of 1 to10 µL min^{-1}. Given a 1:1 mixture of water and either acetonitrile or methanol as a working solution, we estimate the H_2O flux to be 1.67 x 10^{19} to 1.67 x 10^{20} molec min^{-1} through the electrospray capillary. Therefore the ESI capillary provides approximately 7 to 42 % of the water at 50% RH.

The following text has been added to section 3.4: "Assuming a sample flow of 0.8 L min^{-1} and 1 to 10 µL min^{-1} flow through the electrospray capillary, the working solution provides 7 to 42 % of the total water at 50 % RH."

Comment #23:

P19 ln 1: Kumbhani et al. report using a 100 µm ID capillary, while this EESI-TOF uses a 50 µm ID capillary. Authors should revise their statement that the Kumbani et al. capillary has a 5x smaller ID than the EESI-TOF capillary, and revise the subsequent discussion.

Response:

We apologize for the error. The incorrect reference to the dimensions of the Kumbhani et al. capillary has been removed. The remainder of the discussion merely speculates on reasons for the different behavior observed in the two systems, which requires follow-up investigations to resolve and is therefore left unchanged.

Comment #24:

P19 ln 8: please provide a range of expected sizes for the electrospray droplets

Response:

We do not have the capability at present to directly measure the electrospray droplet size distribution. Based on a literature comparison of roughly similar sources, we estimate a droplet mode on the order of 4 to 40 µm. This information has been added to the manuscript.

Comment #25:

P21 ln 29: Add FIGAERO-CIMS to the list of instruments that show thermal decomposition? (see comment above).

Response:

The revised text reads: "As discussed above, current OA measurements used in mobile measurements require a tradeoff between thermal decomposition (extensive for the AMS, minor for FIGAERO-CIMS), ionization-induced fragmentation (AMS, CHARON-PTRMS), or time resolution (FIGAERO-CIMS)."

Comment #26:

P23 ln 7: Change "…for most precursors." To "…for most precursors TESTED."

Response:

This sentence was revised in response to Comment #16 and Reviewer #1 (Comment #6) and now reads: "The EESI-TOF sensitivity to SOA generated from a set of individual precursor gases varies within a factor of 15."

Comment #27:

Figure 5 and discussion: Comparison of several apparent slopes in Fig. 5a with the bars in Fig. 5b seems not to match the relative slopes relationships. E.g. C9H14O7 looks steeper than C9H14O4 and C10H14O4 but the opposite in Fig. 5b (0.4 vs. 0.55 and 0.6). Is this simply due to non-log linear fits being calculated where the regression is highly weighted toward the largest signal data? If that is the case, perhaps also reporting the average ratio (could easily be added to the same bar plot). Other options may be a log-log fit or other regression fitting methods that don't emphasize the high value data points. The point here is that at least inspection of a log-log plot shows that the relative trends shown in Fig. 5b and discussed in the text may not be robust for each ion but rather reflect just a few of the high-signal points for each ion. On the other hand, if the lower signal points are noisier and closer to DLs, then perhaps it is fine to weight those more strongly. Finally, the type of fit (ODR?) and if it was constrained through zero should be reported.

Response:

The apparent discrepancy between the visual appearance of slopes and their actual value is due to non-zero intercepts that are somewhat different for each ion. Lines having the same slope but different intercepts diverge at low values on a log-log plot, with a larger x-intercept corresponding to a visually steeper (but numerically identical) slope. The fits are not significantly influenced by outliers, and must be fit in linear space because they depend on absolute ion counts and not ratio of ion counts to background (as would be the case for a log-log fit). Data are plotted on a logarithmic scale only because ion signals span several orders of magnitude. As a result, we have

not altered Fig. 5. However, we now state in the figure caption that all fits were conducted using ODR and that the intercept is unconstrained.

Comment #28:

Figure 5 and discussion: It would be useful if the authors reported what fraction of the aerosol signal the sum of all the selected ions represents. Most of it? Similarly, it would be useful to show the EESI-TOF and I-CIMS aerosol mass spectra (possibly on a log-scale).

Response:

The requested figure has been added as Fig. 5a. We compare the range *m/z* 100 to 500 for both instruments, with Na^+ and I^- subtracted from the EESI-TOF and FIGAERO-I-CIMS, respectively. The ions selected for comparison ($C_9H_{14}O_x$ and $C_{10}H_{16}O_x$ families) comprise 21 % of the EESI-TOF signal and 19 % of the FIGAERO signal.

The revised text follows: "Figure 5 shows the EESI-TOF and FIGAERO-I-CIMS mass spectra from *m/z* 100 to 500 after subtraction of Na^+ and I^-, respectively. Spectra are normalized such that the sum across the selected *m/z* range is 1. The main features and general trends are similar between the two instruments, although some differences in relative intensity are evident. In addition, the EESI-TOF signal is greatly reduced below *m/z* 150 due to the selected transmission window in the quadrupole ion guides. Figure 5b shows EESI-TOF signals as a function of the FIGAERO-I-CIMS for selected ions, specifically the $[C_9H_{14}O_x]Na^+$ (red) and $[C_{10}H_{16}O_x]Na^+$ (blue) series, which constitute 21% (EESI-TOF) and 19% (FIGAERO-I-CIMS) of the total particle-phase signal."

Comment #29:

Figure 8b: Please include the particle volume distribution standard deviation on Fig. 8b to give a sense of the overlap of sizes, since this experiment was not conducted with monodisperse particles.

Response:

We have added error bars to Fig. 8b, where the error bars denote the mobility diameters corresponding to the half-maxima of the polydisperse particle volume distribution.

Comment #30:

P1, ln 18: Would suggest replacing "SOA compounds" with "identified SOA components" or similar.

Response:

The revised text reads: "…the bulk sensitivity to SOA generated from most tested precursors varies by only a factor of 6."

Comment #31:

P3, ln 23-31: Need references for many of these statements.

Response:

References have been added.

Comment #32:

P4 ln 8: My understanding is that instruments like the ATOFMS and PALMS have much more fragmentation of organic molecules than the AMS. The laser ablation instruments often turn organics into C1+, C2+, and ammonium into NO+. However, as worded this section gives the opposite impression.

Response:

ATOFMS has been used successfully to measure oligomers (Gross et al., 2006), which decompose and/or fragment in the AMS. Therefore at least some combination of compounds/instruments can provide reduced fragmentation/decomposition relative to the AMS, and the text is left unchanged.

Comment #33:

P5 ln 10-11: Text states: "Further, there remain fundamental limits to the detection of highly oxidized compounds, as well accretion products for which there is currently no satisfactory online detection technique." It's not clear what is meant by "fundamental limits" which is vague in this context. Please clarify. Also add "as" between "well" and "accretion".

Response:

We agree that "fundamental" was unclear, and it has been deleted. The identified typo is fixed.

Comment #34:

P9 ln 29: This is perhaps a typo? I have not seen water at 25 C to have more than 18.2 MOhms resistance.

Response:

The typo has been corrected (should have been 18.2 MΩ cm).

Comment #35:

P10 ln 28: this sentence is missing a verb.

Response:

The corrected sentence reads: "Preliminary investigations using an H_2O-only working fluid (with NaI dopant) were also conducted."

Comment #36:

P15 ln 6: a reference to the CIMS strategy described is needed.

Response:

This sentence concludes the discussion of EESI-TOF sensitivity to bulk laboratory-generated SOA and pure compounds, for which the SMPS is used as a reference. Discussion of the CIMS does not begin until the following paragraph. We therefore prefer to leave the text unchanged.

Comment #37:

P16, ln 12-13: Add reference for this statement about matrix effects and ion suppression being common in ESI.

Response:
References added.

Comment #38:
P20 ln 17-18: Remove unneeded "of" and "as" which make the sentence grammatically problematic.

Response:
The revised text reads: "To aid the eye, $[(NaI)_n]Na^+$ clusters are removed; this is done because although the background-subtracted $[(NaI)_n]Na^+$ is close to zero, it is the difference of two high-intensity signals and therefore remains large relative to most ions in the mass spectrum."

Comment #39:
P20 ln12-13 / Fig 9a/b: Please state how mass concentration was determined from SMPS measurements as shown in Fig. 9a/b.

Response:
We assumed an effective density of 1.2 g cm^{-3}.

References

Bertrand, A., Yuan, B., Stefenelli, G., Qi, L., Pospisilova, V., Tong, Y., Sepideh, E., Huang, R.-J., El Haddad, I., Slowik, J. G., and Prevot, A. S. H.: Characterization of fresh and aged solid fuel combustion organic aerosol by extractive electrospray ionization time-of-flight mass spectrometer (EESI-TOF), Environ. Sci. Technol., submitted.

Chen, H., Venter, A., and Cooks, R. G.: Extractive electrospray ionization for direct analysis of undiluted urine, milk and other complex mixtures without sample preparation, Chem. Commun., 19, 2042-2044, 10.1039/b602614a, 2006.

Chen, H., Gamez, G., and Zenobi, R.: What can we learn from ambient ionization techniques?, J. Am. Soc. Mass Spec., 20, 1947-1963, 2009.

Eichler, P., Müller, M., D'Anna, B., and Wisthaler, A.: A novel inlet system for online chemical analysis of semi-volatile submicron particulate matter, Atmos. Meas. Tech., 8, 1353-1360, 10.5194/amt-8-1353-2015, 2015.

Gallimore, P. J., and Kalberer, M.: Characterizing an extractive electrospray ionization (EESI) source for the online mass spectrometry analysis of organic aerosols, Environ. Sci. Technol., 47, 7324-7331, 10.1021/es305199h, 2013.

Gallimore, P. J., Giorio, C., Mahon, B. M., and Kalberer, M.: Online molecular characterisation of organic aerosols in an atmospheric chamber using extractive electrospray ionisation mass spectrometry, Atmos. Chem. Phys., 17, 14485-14500, 10.5194/acp-17-14485-2017, 2017.

Gross, D. S., Galli, M. E., Kalberer, M., Prevot, A. S., Dommen, J., Alfarra, M. R., Duplissy, J., Gaeggeler, K., Gascho, A., Metzger, A., and Baltensperger, U.: Real-time measurement of oligomeric species in secondary organic aerosol with the aerosol time-of-flight mass spectrometer, Anal Chem, 78, 2130-2137, 10.1021/ac060138l, 2006.

Gu, H. W., Chen, H. W., Pan, Z. Z., Jackson, A. U., Talaty, N., Xi, B. W., Kissinger, C., Duda, C., Mann, D., Raftery, D., and Cooks, R. G.: Monitoring diet effects via biofluids and their implications for metabolomics studies, Anal. Chem., 79, 89-97, 10.1021/ac060946c, 2007.

Pejov, L.: Metal cations: a density functional, coupled cluser, and quadratic configuration interaction study, International Journal of Quantum Chemistry, 86, 356-367, 10.1002/qua.10022, 2002.

Qi, L., Chen, M.-D., Stefenelli, G., Pospisilova, V., Tong, Y.-D., Bertrand, A., Hueglin, C., Rigler, M., Ge, X.-L., Baltensperger, U., Prévôt, A. S. H., and Slowik, J. G.: Real-time source quantification of wintertime secondary organic aerosol in Zurich using an extractive electrospray ionization time-of-flight mass spectrometer (EESI-TOF), Atmos. Chem. Phys., 19, 8037-8062, 10.5194/acp-19-8037-2019, 2019.

Rodgers, M. T., and Armentrout, P. B.: Absolute binding energies of sodium ions to short chain alcohols, $C_nH_{2n+2}O$, n = 1-4, determined by threshold collision-induced dissociation experiments and ab initio theory, J. Phys. Chem. A, 103, 4955-4963, 10.1021/jp990656i, 1999.

Stefenelli, G., Lopez-Hilfiker, F. D., Pospisilova, V., Vogel, A., Hüglin, C., Baltensperger, U., Prévôt, A. S. H., and Slowik, J. G.: Source apportionment of ambient organic aerosol by online extractive electrospray ionization time-of-flight mass spectrometry (EESI-TOF), Atmos. Chem. Phys. Discuss., 10.5194/acp-2019-361, 2019.

Zhou, Z. Q., Jin, M., Ding, J. H., Zhou, Y. M., Zheng, J., and Chen, H. W.: Rapid detection of atrazine and its metabolite in raw urine by extractive electrospray ionization mass spectrometry, Metabolomics, 3, 101-104, 10.1007/s11306-006-0050-2, 2007.

An Extractive Electrospray Ionization Time-of-Flight Mass Spectrometer (EESI-TOF) for online measurement of atmospheric aerosol particles.

Felipe D. Lopez-Hilfiker[1,a], Veronika Pospisilova[1], Wei Huang[2], Markus Kalberer[3,4], Claudia Mohr[5], Giulia Stefenelli[1], Joel A. Thornton[6], Urs Baltensperger[1], Andre S. H. Prevot[1], Jay G. Slowik[1]

[1]Laboratory of Atmospheric Chemistry, Paul Scherrer Institute (PSI), 5232 Villigen PSI, Switzerland

[2]Institute of Meteorology and Climate Research, Karlsruhe Institute of Technology, 76131 Karlsruhe, Germany

[3]Department of Chemistry, University of Cambridge, Cambridge CB2 1EW, United Kingdom

[4]Department of Environmental Sciences, University of Basel, 4056 Basel, Switzerland

[5]Department of Environmental Science and Analytical Chemistry, Stockholm University, 106 91 Stockholm, Sweden

[6]Department of Atmospheric Sciences, University of Washington, Seattle, WA 98195, Washington, USA

[a]*Now at*: Tofwerk AG, 3600 Thun, Switzerland

Correspondence to: Jay G. Slowik (jay.slowik@psi.ch)

Abstract

Real-time, online measurements of atmospheric organic aerosol (OA) composition are an essential tool for determining the emissions sources and physicochemical processes governing aerosol effects on climate and health. However, the reliance of current techniques on thermal desorption, hard ionization, and/or separated collection/analysis stages introduces significant uncertainties into OA composition measurements, hindering progress towards these goals. To address this gap, we present a novel, field-deployable extractive electrospray ionization time-of-flight mass spectrometer (EESI-TOF), which provides online, near-molecular (i.e., molecular formula) OA measurements at atmospherically relevant concentrations without analyte fragmentation or decomposition. Aerosol particles are continuously sampled into the EESI-TOF, where they intersect a spray of charged droplets generated by a conventional electrospray probe. Soluble components are extracted, and then ionized as the droplets are evaporated. The EESI-TOF achieves a linear response to mass, with detection limits on the order of 1 to 10 ng m^{-3} in 5 s for typical atmospherically-relevant compounds. In contrast to conventional electrospray systems, the EESI-TOF response is not significantly affected by a changing OA matrix for the systems investigated.~~, while a~~A slight decrease in sensitivity in response to increasing absolute humidity is observed for some ions. Although the relative sensitivities to a variety of commercially available organic standards vary by ~~approximately~~ more than a factor of 30, the bulk sensitivity to ~~most~~ SOA generated from individual precursor gases ~~compounds~~ varies by only a factor of ~~6~~15. Further, the ratio of compound-by-compound sensitivities between the EESI-TOF and an iodide adduct FIGAERO-CIMS vary by only ±50%, suggesting that EESI-TOF mass spectra indeed reflect the actual distribution of detectable compounds in the particle phase. Successful deployments of the EESI-TOF for laboratory environmental chamber measurements, ground-based ambient sampling, and proof-of-concept measurements aboard a research aircraft highlight the versatility and potential of the EESI-TOF system.

1. Introduction

Aerosol particles adversely affect respiratory and cardiovascular systems, scatter and absorb radiation, influence cloud formation processes and properties, provide surfaces for heterogeneous reactions, and affect trace gas concentrations by providing an adsorptive medium for semi-volatile gases. As a result, aerosols have a significant effect on public health, climate, and overall atmospheric reactivity. Of particular importance are aerosol particles smaller than 1 μm in diameter, a significant and ubiquitous fraction of which is secondary organic aerosol (SOA) formed from atmospheric reactions of organic gases (Hallquist et al., 2009; Jimenez et al., 2009). The sources, aging, and chemical properties of SOA remain highly uncertain, and these uncertainties can lead to large errors between modeled and measured aerosol loadings (Volkamer et al., 2006). These errors limit our ability to predict future changes in aerosol particle composition and concentration under a warming climate and to link SOA to its atmospheric emission sources. To develop adequate model parameterizations of organic aerosol (OA) and its formation, growth, and loss, there remains a need to improve source apportionment capabilities and to identify chemical mechanisms governing the conversion and partitioning of organic compounds between gas and particle phase. Measurements of specific chemical tracers on timescales similar to the typical variability in emissions, photochemical activity, and meteorology, approximately minutes to hours, would improve source apportionment, mechanistic studies, and characterization of bulk molecular properties such as the distribution of average oxidation state across carbon number (Kroll et al., 2011) against mechanistic photochemical models.

The chemical complexity of OA makes highly time-resolved, chemically-specific measurements extremely challenging. OA consists of thousands of individual components, many of which are present at only trace amounts (Goldstein and Galbally, 2007). Most organic aerosol chemical speciation to date has come from offline analysis of filter samples. Offline samplers typically concentrate particles on a filter or impactor for 2-24 hours, after which particles are extracted or thermally desorbed for offline chemical analysis (Hallquist et al., 2009). The main disadvantages of offline techniques are their low time resolution, which is much slower than many atmospheric processes, and the potential for chemical changes due to evaporation, adsorption, and/or reaction during sample collection, transfer, and/or storage (Turpin et al., 1994; Subramanian et al., 2004; Timkovsky et al., 2015; Kristensen et al., 2016). The extraction process is also time consuming and can introduce additional artifacts into the measurements (e.g. decomposition during

derivatization or hydrolysis in aqueous solutions). A recent study addresses the issue of low time resolution and reaction on the collection substrate by collecting samples at 5 min time resolution using a particle-into-liquid sampler (PILS) coupled to collection vials on a rotating carousel, followed by offline ultra-performance liquid chromatography/electrospray ionization quadrupole time-of-flight mass spectrometry (UPLC/ESI-Q-TOFMS) analysis (Zhang et al., 2015; Zhang et al., 2016). This approach yielded time-resolved molecular speciation for water-soluble components, but remains subject to sample transfer and storage artifacts.

Traditional techniques for rapid online measurements of OA without sample handling rely on the combination of mass spectrometry with thermal desorption. Most single particle instruments, e.g. ATOFMS (Gard et al., 1997), SPLAT (Zelenyuk and Imre, 2005), and PALMS (Murphy et al., 2006), utilize simultaneous laser desorption/ionization, which is not quantitative due to matrix effects and can also result in fragmentation of organic molecules. In contrast, the Aerodyne aerosol mass spectrometer (AMS) utilizes a high vaporization temperature (600 C) and electron ionization (EI, 70 eV) to remain quantitative, but at the cost of extensive thermal decomposition and ionization-induced fragmentation (Canagaratna et al., 2007). More recently, the CHARON-PTR couples an aerodynamic particle lens with a heated inlet and a softer ionization scheme (via proton transfer reaction) for measurements of particles between 100 and 750 nm (Eichler et al., 2015). This provides improved chemical speciation for some atmospherically-relevant compounds; e.g. oleic acid and 5α-cholestane (Müller et al., 2017). However, proton transfer is too energetic for studies of the oxygenated compounds characteristic of SOA; for example, only ~10% of *cis*-pinonic acid is detected as the parent ion $[M]H^+$, with the rest distributed across several fragments. Extensive fragmentation in the CHARON-PTR also occurs for oxygenated primary compounds such as levoglucosan limiting its usefulness in mechanistic studies. Another recent development, the AeroFAPA-MS (aerosol flowing atmospheric-pressure afterglow mass spectrometer) (Brüggemann et al., 2015; Brüggemann et al., 2017) couples thermal vaporization with ionization by the outflow of a low-temperature plasma. The AeroFAPA-MS has detection limits suitable for ambient aerosol measurements and when detecting ions in negative mode is subject to significantly less fragmentation than is PTR, but due to the variety of ions produced in the plasma is subject to various competing ionization pathways, complicating spectral interpretation and quantitative analysis.

The need for molecular-level information (without ionization-induced fragmentation) led to the development of a number of semi-continuous online measurements that follow a general two-step collection and analysis procedure. Aerosol is typically collected for 10-60 minutes either by impaction or on a filter, then thermally desorbed for gas chromatography with prior online derivatization (Isaacman et al., 2014), proton transfer reaction mass spectrometry (PTR-MS) (Holzinger et al., 2010), or chemical ionization mass spectrometry (CIMS) (Lopez-Hilfiker et al., 2014). These techniques offer significantly improved chemical resolution relative to online systems, but remain subject to thermal decomposition during desorption (though to a lesser degree than the AMS), as well as reaction or partitioning effects on the collection substrate. In some systems which feature a temperature ramp, thermal decomposition products can be identified as such, although links to the parent molecules are unclear (Lopez-Hilfiker et al., 2015). Further, there remain ~~fundamental~~ limits to the detection of highly oxidized compounds, as well as accretion products for which there is currently no satisfactory online detection technique. Finally, the time delay between aerosol collection and detection can compromise detection of fast intra-particle reactions (Pospisilova et al., submitted). Therefore, there remains a need for fast, online aerosol analysis without decomposition or fragmentation.

Electrospray ionization (ESI) is a well-known method for transferring low volatility, high molecular weight molecules (e.g. proteins and peptides) into gas phase ions without the need for direct heating. ESI has been successfully coupled to mass spectrometry for offline analysis of atmospheric aerosol both by direct infusion of aerosol extracts (Reemstsma et al., 2006; Zhang et al., 2011) and surface sampling techniques (Laskin et al., 2010; Roach et al., 2010). Extractive electrospray ionization (EESI) is a technique that couples the advantages of ESI with online continuous measurement (Chen et al., 2006). In extractive electrospray ionization, a solvent is delivered through a conventional electrospray probe generating a plume of charged electrospray droplets. The primary spray is directed into a sample flow of gases and/or aerosol whereby the collision between aerosol and electrospray droplets results in the extraction of the soluble components into the bulk electrospray droplet. During the rapid evaporation of the solvent from the electrospray droplets, surface charge is concentrated and ions are ejected into the gas phase, presumably by the Coulomb explosion mechanism (Kebarle and Peschke, 2000). These ions are then sampled directly into a mass spectrometer for analysis.

There have been several previous attempts to apply extractive electrospray ionization to atmospheric gas and particle studies. However, the detection limits achieved by these techniques are one or more orders of magnitude too high to be useful in the atmosphere or for laboratory experiments at atmospherically-relevant concentrations (i.e. ~1-10 μg/m^3). Doezema et al. (2012) identified a limited number of compounds in α-pinene SOA at aerosol mass loadings of 1500-2500 μg m^{-3}. Ambient ESI, a conceptually similar technique to EESI, detected particle-phase organic compounds, including some oligomers, at 26 μg m^{-3} of SOA from α-pinene ozonolysis, although instabilities in the mass analyzer precluded quantitative analysis (Horan et al., 2012). A more recent EESI system (Gallimore and Kalberer, 2013; Gallimore et al., 2017) attained individual compound detection limits of ~1 μg m^{-3} for 100 s integration (M. Kalberer, private communication), which were further reduced to as low as 0.25 μg m^{-3} using tandem mass spectrometry (MS^2) and collisionally-induced dissociation (CID). While a significant improvement compared to previous work, these detection limits remain insufficient for most atmospheric systems, where even the most abundant compounds in OA are typically present in concentrations of 10-100 ng m^{-3}. However, EESI was shown to be linear over several orders of magnitude, independent of particle size or morphology up to 200 nm, and reproducible, highlighting its potential benefits for atmospheric OA analysis with soft ionization and without thermal desorption (Gallimore and Kalberer, 2013).

Here we present the development and characterization of a novel EESI interface coupled to a portable high-resolution time-of-flight mass spectrometer (EESI-TOF). Our design, while conceptually similar to previous EESI work, provides detection limits as low as 1 ng m^{-3} at 1 Hz through a combination of source optimization and efficient ion transfer into and through the mass spectrometer. We present comprehensive characterization of the source, including sensitivity, linearity, time response, as well as water vapor and matrix sampling effects. We also present proof of concept measurements from the reaction of α-pinene and ozone in a laboratory flow tube, ambient measurements in Zurich, Switzerland, and airborne wildfire measurements in the central United States.

2. Instrument ~~Description~~description

In brief, the EESI-TOF system consists of a custom built EESI inlet and ionization source coupled to a commercially available mass spectrometer (APi-TOF, Tofwerk, Thun, Switzerland). In addition to the physical inlet design, selection of working fluid and ionization scheme are critical for optimal EESI-TOF operation.

2.1.EESI design

The EESI source was developed with the specific goal to measure OA at a near-molecular level (with "near-molecular" here defined as the determination of a molecular formula, without direct structural information or isomeric separation), however it can more generally be applied to gas or combined gas/particle measurements. Figure 1 shows a schematic of the main components of the EESI. For particle measurements, the instrument automatically alternates between direct sampling and sampling through a Teflon filter with a 1 µm pore size (Fig. 1, orange). The difference between the direct and filter blank measurements is the background-corrected particle-phase signal. For the proof-of-concept deployments discussed in Section 4, this filter was replaced with a nylon cartridge filter (9933-11-NQ, Parker Balston, Lancaster, NY, USA), which performed similarly. Particles and gases enter the EESI source through a 6 mm inner diameter (ID) 5 cm long multi-channel extruded carbon denuder (Fig. 1, black) at a flow rate of 0.7 to 1.0 L min^{-1}. ~~At this flow rate, the denuder removes most gas phase species with high efficiency (e.g. pinonic acid > 99.6%).~~ The denuder is housed in a stainless steel tube that can be biased relative to the entrance of the mass spectrometer, but is typically set to ground. The denuder improves instrument detection limits by reducing the gas-phase background. In addition, it removes from the particle flow any sticky gases that may be lost to the filter and otherwise misclassified as particulate material.

The denuder is very similar to that used for the CHARON-PTRMS, where it removes methanol, acetonitrile, acetaldehyde, acetone, isoprene, methylethylketone, benzene, toluene, xylene, 1,3,5-trimethylbenzene, and α-pinene with >99.9999% efficiency (Eichler et al., 2015). Our experiments show >99.95% removal for pinonic acid, and no detectable breakthrough in the chamber and field experiments presented in Section 4, which were conducted at OA concentrations up to approximately 10 µg m^{-3} with the denuder not requiring regeneration for at least 2 weeks. For smog chamber experiments on wood and coal-burning emissions at higher concentrations (20 to 200 µg m^{-3}, 1 experiment of 3-4 h per day) (Bertrand et al., submitted), the denuder was regenerated every 2 to 3 days, when a slower response time was observed on switching between

the direct sampling and filter blank measurements. This suggests a higher capacity denuder should be used for continuous sampling under polluted conditions.

After the sample passes through the denuder, particles collide with the primary electrospray droplets in a laminar sample flow and the soluble components are extracted. The electrospray is generated by a commercially available 360 μm OD untreated fused silica capillary with an inner diameter of 50 μm (BGB Analytik AG, Boeckten, Germany), with no further treatment. The ESI probe is positioned approximately 1 cm away from the mass spectrometer inlet. A high voltage liquid junction and electrospray fluid reservoir (80 mL) is used to deliver the solvent to the ESI capillary. We find that fluid flow rates between 0.1-10.0 μL/min leads to the formation of a stable primary spray without requiring a sheath gas. Initially, the ESI working fluid was delivered using a commercially available syringe pump (KD Scientific, Holliston, MA, USA) via a 250 μL syringe. However, a combination of unstable fluid delivery rates (pulsed flow) and limited run time (i.e. several hours) led to the replacement of the syringe pump with a high precision pressure regulator for fluid flow (MFCS-EZ 1000 mbar, Fluigent, Inc., Lowell, MA, USA) coupled to a large liquid reservoir. This system allows continuous solvent delivery for months at a time and ensures ultra-stable fluid flow rates.

The droplet-laden flow enters the mass spectrometer through a heated stainless steel capillary to evaporate excess electrospray solvent and facilitate efficient ion formation (Figure 1, blue). The inlet flow rate is ~~between 0.7 and 1.0 L min^{-1} and~~ determined by the capillary temperature and as noted above is between 0.7 and 1.0 L min^{-1}. We use a commercially available stainless steel capillary (0.5 mm inner diameter (ID), 1/16" OD 70 mm long; VICI AG International, Schenkon, Switzerland), which is housed in a conical capillary heater manifold fabricated from aluminum. A tight fit between the heating manifold and capillary helps to ensure uniform heating and efficient heat-transfer to the capillary from the heater block controlled by two cartridge heaters. The ~~capillary manifold is~~heaters are operated at ~250 °C to ensure that electrospray droplets evaporate during the ~1 ms transit through the capillary tube. Note that the combined effects of gas expansion, solvent evaporation, capillary temperature, finite heat transfer (from both cartridge heater to capillary walls and capillary walls to gas), and short residence time results in a sample gas of significantly lower absolute temperature than the 250 °C heater temperature would suggest. The spray probe and assembly is coupled to the mass spectrometer via a PTFE manifold (Fig. 1, green), which thermally isolates the sample flow from the heated capillary manifold (Fig. 1, blue).

An aluminum heat sink plate compresses the EESI mounting manifold to the sample cone of the capillary inlet and draws heat away from the sample flow using a small fan. In this way, the sample flow remains unheated until after extraction into the ESI droplets, minimizing volatilization of labile particle phase components and thermal decomposition.

Evaporation of the charged droplets yields ions via the Coulomb explosion mechanism. These ions are analyzed by a portable high-resolution time of flight mass spectrometer with an atmospheric pressure interface (APi-TOF, Tofwerk, Thun, Switzerland), which has been described in detail previously (Junninen et al., 2010) but modified with a heated capillary inlet. We find that maximum ion transmission is achieved by maximizing the flow rate into the mass spectrometer, which for our pumping configuration is nominally 1 L min^{-1} at standard temperature and pressure (STP).

2.2. Extraction and ionization

Conceptually, the EESI solution consists of two components: (1) a working fluid for aerosol extraction and spray formation and (2) a dopant for control of ionization pathways. Note that changing one or both of these components alters the set of detectable compounds, increasing the versatility of the EESI-TOF system. In this initial study, we focus on efficient, stable detection of a broad range of organic compounds, with an emphasis on oxygenated SOA. The working fluid and ionization dopant were optimized for the detection of a-pinene ozonolysis products.

Regardless of the working fluid, the electrospray solution is doped with 100 ppm NaI to promote ionization by sodium ion attachment (Na^+), and suppress alternative pathways such as proton transfer ($[M]H^+$), formation of adducts with other ions (e.g. Li^+ or K^+), charge transfer, and proton abstraction ($[M-H]^-$). Positive ion detection is therefore employed. In principle, any compound may be added to the ESI working fluid to control the ionization process, provided that the ion-adduct binding energies are sufficiently strong to survive droplet evaporation. (For example, detection of I^- adducts in negative mode has so far been unsuccessful, as the $[M]I^-$ adducts dissociate into [M] and I^-, presumably during transit through the heated capillary). However, we find that Na^+ ions generate strong enough molecular adducts with a wide range of organic molecules present in atmospheric aerosol, including sugars, acids, alcohols, organic nitrates, and highly oxidized multifunctional molecules. In principle, Li^+ likely provides stronger adducts and

may thus facilitate quantification and improve detection of weakly bound species (Zhao et al., 2017). However, Na^+ also has the advantage of only a single peak (no isotopes), which simplifies peak identification and reduces spectral clutter. The detected molecular classes include nearly all compounds present in secondary organic aerosol, with the important exception of organosulfates, which are typically detected as negative ions in electrospray-based studies (Surratt et al., 2008). This ionization scheme is also not sensitive to non-oxygenated compounds such as alkanes, alkenes, and aromatic hydrocarbons. The detectable species are observed exclusively as adducts with Na^+. Indeed, the only molecule in ambient or laboratory aerosol that we have identified as ionizing without Na^+ attachment is nicotine, where the ionization instead proceeds via net proton transfer, yielding $[M]H^+$ (Qi et al., 2019; Stefenelli et al., 2019). It may be that other reduced nitrogen species follow a similar pathway.

Additional benefits of the Na^+ dopant include provision of (1) an internal measure of spray stability and (2) reference ions for *m/z* calibration. For the former, we typically monitor the $[NaI]Na^+$ ion (*m/z* 172.883), as for some experiments it is desirable to set the quadrupole guides to block transmission from low *m/z* ions (including Na^+ and working fluid-related signals) to increase detector lifetime. For *m/z* calibration, we utilize a series of $[(NaI)_n]Na^+$ clusters, which are well-spaced across the entire *m/z* of interest for ambient aerosol and also have a strong negative mass defect, reducing interferences with organic analytes.

For the ESI working fluid, mixtures of acetonitrile (ACN) (HPLC grade, ≥99.9% purity, Sigma-Aldrich, St. Louis, USA) and methanol (MeOH) (UHPLC-MS LiChrosolv, ≥99.9% purity, Sigma-Aldrich, St. Louis, USA) in a variable ratio with ultrapure water (~~19~~18.2 MΩ cm, total-organic carbon < 5 ppb) were selected for testing; all solutions included the 100 ppm NaI dopant. The solvent blend was optimized with the goals of (1) maximizing the overall OA detection (extraction + ionization) efficiency and (2) generating a spray that is stable over long timescales. We tested a 1:1 MeOH:H_2O mixture and compared this to ACN:H_2O mixtures, as these are the two most common electrospray solvents used in traditional analysis (HPLC and direct infusion ESI) and should have a high overall extraction efficiency of OA. Both solvent blends formed stable electrospray as determined by the stability of detected ion currents over long timescales (days to weeks) and gave similar sensitivities for products from α-pinene SOA.

We found that the MeOH:H_2O spray produces significant background peaks throughout the spectrum, presumably due to impurities, which are efficiently ionized by the primary electrospray probe. These background signals increase detection limits and complicate interpretation of blank subtraction during the EESI process. Significant effort to ensure the cleanliness of the primary solution is therefore of critical importance for maintaining low detection limits. We found that using a mixture of ACN:H_2O for the primary spray generation reduced these backgrounds by approximately an order of magnitude, leading to a net decrease in detection limits. This reduction could simply be due to a more pure acetonitrile solvent compared to methanol. We observe that the effective binding energy of the acetonitrile adduct with sodium $[(ACN)_n]Na^+$~~)~~ is significantly stronger than that of methanol (Rodgers and Armentrout, 1999; Pejov, 2002). Irrespective of solvent purity, we expect this stronger binding energy to yield a somewhat cleaner spectrum by suppressing subsequent ionization processes. In our test system (α-pinene SOA), we observe the ACN:H_2O working fluid can yield clusters of analyte molecules with acetonitrile (i.e., $[M(ACN)]Na^+$), with abundances on the order of 10% of the parent ion ($[M]Na^+$). This effect remains to be characterized in other chemical systems. Note that the cluster abundance depends on the electric fields in the interface and capillary temperature, both of which can be adjusted. Increasing either will decrease the cluster abundance, however at some point the additional energy required to decluster solvent from the organic adducts will reach the binding energy of the organic sodium adducts, thereby reducing overall sensitivity. Note that the sensitivity vs. declustering tradeoff does not affect all species equally and is of greatest importance for the most weakly bound adducts. Herein we present results using mostly the MeOH:H_2O spray, unless otherwise explicitly noted.

Preliminary investigations using an H_2O-only working fluid (with NaI dopant) were also conducted. This working fluid is of interest because it yields backgrounds even lower than those of the ACN:H_2O mixture. However, in our preliminary tests the primary ion count for H_2O is also lower by a factor of ~20 relative to ACN:H_2O. Further, unlike the MeOH:H_2O and ACN:H_2O sprays, sampling of ~30 to 35 μg m^{-3} of aerosol from re-nebulized ambient filter extracts resulted in a 10 to 15% decrease in the primary ion signal from the H_2O spray, increasing the possibility of ion suppression artifacts or other non-linear behavior. Therefore, while the H_2O spray may be of interest for background-limited applications, it cannot be assumed to perform similarly to the MeOH:H_2O and ACN:H_2O sprays, and detailed characterization is needed.

3. Performance and characterization

The EESI-TOF performance was assessed using a variety of single components and atmospherically relevant multi-component aerosol. We focus on assessing sensitivity and detection limits, linearity of response to aerosol mass, and the effects of changes in the OA matrix or water vapor concentrations on EESI-TOF performance.

3.1. Test aerosol generation and basic operation

To characterize and optimize EESI-TOF performance we used both single-component aerosol generated by a conventional nebulizer system as well as multi-component aerosol produced from the reaction of α-pinene and O_3 in a flowtube, the configuration of which is described in detail elsewhere (Molteni et al., 2018). The α-pinene is delivered by a diffusion vial from a pure liquid at room temperature into a carrier gas flow of 1-10 L min^{-1} of zero air at the entrance of the flow tube. O_3 (0.25-5 ppmv) is produced from a commercially available ozone generator and is mixed into the main flow at the flowtube entrance. This leads to the prompt formation of SOA during the (~1-5 min) residence time in the flow tube. While SOA generated under such conditions is likely not entirely representative of real atmospheric conditions, it contains a suite of highly oxygenated organic monomers, dimers, and higher-order oligomers and therefore provides a useful test aerosol matrix beyond what can be interrogated using a single compound. In this way, we are able to provide a more comprehensive characterization of instrument performance.

Figure 2 shows a sample time series of $[C_{10}H_{16}O_8]Na^+$ measured in SOA generated from α-pinene ozonolysis, with an expanded view shown in the lower panel. Over this measurement period, maximum SOA concentrations reach approximately 30 μg m^{-3}. Here the EESI-TOF alternates between 3 min of direct sampling and a 30 s filter blank, denoted by red circles. The background concentration measured during the filter blank is a small fraction of the total signal and is stable over time, typical of our experience for laboratory and atmospheric concentrations of up to at least 100 μg m^{-3}. The system rapidly responds to filter actuation, with the signal equilibrating on the order of 5 s. Interposing the filter into the sampled flow causes a small pressure drop, which may slightly perturb the spray; deviations in the $[NaI]Na^+$ signal of up to 2% are typical.

Fundamentally, the EESI-TOF measurement is in terms of the ion flux reaching the detector (Hz), as shown on the left axis of Fig. 2. However, in most studies the particle phase is ~~typically~~

described in terms of mass for both absolute and relative concentrations, making it desirable to also obtain a mass-related metric from the EESI-TOF measurements. In principle, the EESI-TOF ion signal for a molecule *x* can be converted to a mass concentration according to Eq. (1):

$$Mass_x = I_x \left(\frac{MW_x}{EE_x * CE_x * IE_x * TE_{m/z}} \right) * \frac{1}{F} \quad (1)$$

Here $Mass_x$ denotes the ambient mass concentration of molecule *x*, I_x is the measured ion flux, *F* is the inlet flowrate (0.7 to 1.0 L min^{-1}, depending on inlet capillary temperature), and MW_x is the molecular weight of *x*. Note that MW_x does not generally correspond to the *m/z* at which *x* is measured, which is typically an Na^+ adduct of *x*. The remaining terms address the probability that a molecule exposed to the electrospray is detected as an ion. The probability that a molecule dissolves in the spray is defined as the extraction efficiency (EE_x). The probability that the analyte-laden droplet enters the inlet capillary is defined as the collection efficiency (CE_x). Ions are generated as the droplets evaporate; the probability that an ion forms and survives declustering forces induced by evaporation and electric fields is defined as ionization efficiency (IE_x). Finally, the probability that a generated ion is transmitted to the detector is defined as transmission efficiency ($TE_{m/z}$) and is independent of chemical identity, depending only on *m/z*. We cannot at present distinguish between effects of the four efficiency terms, and so define their product as an empirically-determined compound-dependent response factor (RF_x), such that:

$$Mass_x = I_x * \frac{MW_x}{RF_x} * \frac{1}{F} \quad (2)$$

The RF_x parameter denotes the total number of ions detected per molecule incident to the spray (i.e. probability that a sampled molecule is detected). ~~In the absence of~~Assuming no fragmentation or decomposition, ~~which has not been observed for any system presented herein,~~ RF_x may be equivalently treated in terms of mass. At present, RF_x has been measured only for a few compounds, and we do not have a reliable parameterization for the many unknowns sampled in laboratory and atmospheric aerosol. Nevertheless, we can arrive at a closer approximation of sampled mass by applying MW_x to calculate the mass flux of *x* to the detector (MF_x):

$$MF_x = I_x * MW_x \quad (3)$$

The quantity MF_x is used herein for assessment of bulk properties (e.g. comparison of total EESI-TOF signal to external mass measurements and investigation of relative composition). For reference, we show on the right axis of Fig. 3 the MF_x (in attograms (10^{-18} g) per second, ag s^{-1})

corresponding to the measured I_x; however, for the remainder of the basic characterization experiments presented herein we show instead the directly measured I_x, which is the actual quantity measured by the instrument.

3.2. Linearity and sensitivity

To assess EESI-TOF linearity, single-component aerosols were nebulized and sampled simultaneously by the EESI-TOF and a scanning mobility particle sizer (model 3080 differential mobility analyzer and model 3022 condensation particle counter, TSI, Inc., Shoreview, MN, USA). Figure 3 shows the background-subtracted EESI-TOF signal as a function of calibrant mass for two model compounds: raffinose ($C_{18}H_{32}O_{16}$, a surrogate for α-pinene dimers) and dipentaeryrithritol ($C_{10}H_{22}O_7$, a surrogate for isoprene accretion products). Concentrations vary from approximately 1 to 1000 ng m^{-3}, thereby covering an atmospherically relevant range of concentrations for single components. In both cases, the molecular species is detected exclusively as adducts of the original molecule with Na^+, and both compounds exhibit a linear response to mass in agreement with previous work (Gallimore and Kalberer, 2013). Critically, individual component concentrations of only 10 ng m^{-3} are readily detectable by the EESI-TOF (5 s average). Detection limits based on 3-σ variation of adjacent filter blank measurements (i.e. the instrument and spray background) are on the order of a few ng m^{-3}. These detection limits improve on the most sensitive previously reported EESI-based aerosol systems by approximately 2 orders of magnitude (or 2-3 orders of magnitude for non-MS^2 systems) (Doezema et al., 2012; Horan et al., 2012; Gallimore and Kalberer, 2013) and are sufficient to allow for the first time the detection of OA components in real atmospheric aerosol. Note that these improved detection limits represent the performance of the entire EESI-TOF instrument relative to previous instruments, and we cannot disentangle the contributions of the ionization unit and MS detector.

The different slopes observed between raffinose and dipentaerythritol (4.49 vs. 108 Hz / μg m^{-3}) correspond to response factors of RF_{raff} = 1.88 x 10^{-8} ions $molec^{-1}$ and RF_{dpe} = 2.93 x 10^{-7} ions $molec^{-1}$, assuming spherical particles with the material density of the pure component. This implies significant differences in the relative sensitivity of the EESI-TOF to different compounds, although as shown later in Fig. 4 dipentaerythritol is an extreme case. Differences are in RF_x expected, however, and may arise from thermodynamic and/or kinetic limitations on extraction efficiency,

as well as ion-adduct binding energies. (In principle, ion suppression, matrix effects, and multiple ionization pathways can also affect sensitivity, though as discussed above and in the next section we do not believe that these issues significantly affect the EESI-TOF). In Fig. 4, we compare the RF_x of a suite of saccharides, polyols, and carboxylic acids, as well as bulk SOA generated by reaction of precursor VOCs with OH radicals in a potential aerosol mass (PAM) flow reactor (Lambe et al., 2011). Because the absolute sensitivity of the EESI-TOF depends on instrument setup (spray optimization, mass spectrometer tuning, etc.), we define a relative response factor (RRF_x), using sucrose as a reference:

$$RRF_x = \frac{RF_x}{RF_{sucrose}} \quad (4)$$

Sucrose is chosen as a reference due to its ease of use (i.e. low volatility and high water solubility) and because it is the standard which we have measured most frequently. The pure component RF_x are calculated from SMPS distributions assuming spherical particles with the material density of the pure component, while the SOA RF_x are calculated from the total organic mass of a co-located AMS. Figure 4 primarily shows RF_x determined with the MeOH:H_2O system, although a few ACN:H_2O measurements are included as well.

Several features are evident from Fig. 4. There is a strong decrease in saccharide sensitivity with increasing molecular weight, with the sensitivity of glucose (6 carbon atoms) being nearly 10 times greater than that of glycogen (24 carbon atoms). The relative sensitivities of carboxylic acids and polyols each also span approximately an order of magnitude, although for these classes a clear molecular weight dependence is not observed. The measured polyols also appear to have somewhat higher sensitivities than the other molecular classes, although this feature should be interpreted with caution due to the small number of compounds tested.

The measured SOA mostly follows a trend of decreasing sensitivity with decreasing molecular weight of the precursors, although the high sensitivity of 1,3,5-trimethylbenzene makes it a slight outlier. Calculation of these sensitivities requires the assumption of SOA molecular weights, which were estimated from the EESI-TOF mass spectrum to be 181 g mol^{-1} (benzene), 173 g mol^{-1} (phenol), 195 g mol^{-1} (toluene), 209 g mol^{-1} (naphthalene), 199 g mol^{-1} (α-pinene), and 220 g mol^{-1} (1,3,5-trimethylbenzene). ~~Neglecting benzene (which is an outlier), t~~The RRF_x observed for the SOAs span a much smaller range than do the pure components~~, (~~i.e. a factor ~~6~~ 15 between ~~phenol~~ benzene and 1,3,5-trimethylbenzene compared to a factor of ~30 between citric acid and

dipentaerythritol (note that the range of RRF_x for pure components is an underestimate, as some pure components must have an *RRF* at least as low as benzene, which is itself a factor of 3 lower than citric acid)). The smaller RRF_x range exhibited by the SOA experiments is expected given that each value represents the mean *RRF* of a complex mixture and is more consistent with ambient observations, where we do not observe major composition-dependent variations in overall EESI-TOF sensitivity to bulk ambient OA (Qi et al., 2019; Stefenelli et al., 2019). However, direct calibration is clearly advisable for compounds for which absolute quantification is desired. Further, for aerosol of unknown composition the possibility of multiple isomers (potentially having significantly different RRF_x) must be considered.

The SOA species shown in Fig. 4 are comprised of many individual compounds, and it is highly desirable to constrain their relative concentrations and thus RRF_x. However, direct calibration of every compound is not feasible due to the large number of species present; in addition, many SOA compounds are not commercially available and cannot be readily synthesized. Therefore, to better understand the relative sensitivities of the individual ions, we utilize as a reference the well-characterized FIGAERO-I-CIMS (filter inlet for gases and aerosols, coupled to iodide chemical ionization mass spectrometry) (Lopez-Hilfiker et al., 2014). The FIGAERO collects particles for 30 min, after which a 45 min thermal desorption program is applied and the resulting organic vapor is detected by I-CIMS. Reaction rates in the FIGAERO-I-CIMS are collision-limited, which in conjunction with ion-adduct binding energies and operational characterization of the declustering potential within the ion transfer optics allows estimation of the sensitivity of the instrument to compounds for which standards do not exist. A direct compound-to-compound comparison between the EESI-TOF and FIGAERO-I-CIMS thus allows us to assess how RRF_x obtained by the EESI-TOF compare to an ionization/detection scheme that can be well-described theoretically in terms of fundamental principles (Iyer et al., 2016; Lopez-Hilfiker et al., 2016).

As a test aerosol, we again select SOA from α-pinene ozonolysis, for which many of the product compounds are detected at or near the collision limit by the FIGAERO-I-CIMS. Figure 5a shows EESI-TOF signals as a function of the FIGAERO-I-CIMS for selected ions, specifically the $[C_9H_{14}O_x]Na^+$ (red) and $[C_{10}H_{16}O_x]Na^+$ (blue) series. Although this comparison is shown on a logarithmic scale due to the range of signal intensities recorded, strong linear correlations are observed for every ion. Moreover, a single line can reasonably describe the EESI-TOF vs. FIGAERO-I-CIMS correlation, regardless of ion identity. This is further highlighted in Fig. 5b5c,

where the slopes of every ion from the comparison in Fig. ~~5a~~ 5b are shown; the spread of slopes describes the range of relative sensitivities in the EESI-TOF relative to the FIGAERO-I-CIMS. The mean slope is 0.51, with a standard deviation of 0.11, indicating that the instrument-to-instrument sensitivity typically varies by only ±20%, and all ions are within ±40% of the mean. Also of note is a slight reduction in the relative sensitivity of the EESI-TOF to the FIGAERO-I-CIMS for the smaller $[C_9H_{14}O_x]Na^+$ series (0.45 ± 0.09) compared to $[C_{10}H_{16}O_x]Na^+$ (0.57 ± 0.08); however, additional measurements are needed to validate this trend. In all, the strong correlation of the EESI-TOF with the collision-limited FIGAERO-I-CIMS suggests that the FIGAERO-I-CIMS strategy of drawing on a fundamental limit to parameterize sensitivity to unknown compounds may likewise be applicable to the EESI-TOF. ~~Further, the correlation indicates that the spectral patterns observed in the EESI-TOF likely reflect to a large degree the actual distribution of compounds in the particle phase.~~

3.3. Matrix effects

Matrix effects and ion suppression processes are common in direct infusion electrospray sources, introducing non-linear responses to analyte concentration and impeding quantification efforts (Stüber and Reemtsma, 2004; Cappiello et al., 2008; Furey et al., 2013). We therefore characterized EESI-TOF sensitivity to a test compound (dipentaerythritol) in the presence of a complex and variable particle-phase organic matrix produced from α-pinene ozonolysis, used again here as a surrogate for the multi-component aerosol particles present in the atmosphere. Dipentaerythritol was chosen as a reference because it does not evaporate during transit through the flow tube, is relatively unreactive, and has a chemical formula ($C_{10}H_{22}O_7$) not found in α-pinene ozonolysis products (maximum of 18 hydrogen atoms~~s~~ for a C_{10} molecule). A constant concentration of pure dipentaerythritol particles was introduced into the flow tube, and coated with SOA formed from α-pinene ozonolysis, generated as described above. Coating thickness was controlled by varying the O_3 concentration. The initial dipentaerythritol particles are approximately 20 nm in diameter and increase to ~70 nm by coating with α-pinene SOA, corresponding to approximately 75 μg m^{-3} of SOA. At these high SOA concentrations, the α-pinene ozonolysis reaction produces sufficient concentrations of low-volatility organics to induce nucleation, which competes with the dipentaerythritol test particles as a surface for condensing

SOA. At the maximum SOA concentration, analysis of the SMPS size distributions shows that approximately 40% of the mass corresponds to coated dipentaerythritol, and 60% to nucleated α-pinene SOA.

A change in the measured concentration of dipentaerythritol in response to the SOA coating would indicate a matrix-dependent instrument response. Figure 6 shows the measured dipentaerythritol signal ($[C_{10}H_{22}O_7]Na^+$) as a function of $[C_{10}H_{16}O_7]Na^+$, a major ion in α-pinene SOA that is approximately proportional to the total SOA mass. Measurements are colored by time. Even at the thickest coatings, the dipentaerythritol signal is unaffected, indicating that particle-phase matrix effects do not significantly affect the measurement. Although these results are obtained from a single test system, they are consistent with the general trend of matrix effects in EESI studies that are negligible or strongly suppressed relative to conventional electrospray measurements (Chen et al., 2006; Gu et al., 2007; Zhou et al., 2007; Chen et al., 2009). In addition, we find that OA signals measured by the EESI-TOF are well correlated with AMS measurements (e.g. total measurable OA, source apportionment factors, tracer ions) (Qi et al., 2019; Stefenelli et al., 2019). This suggests that EESI-TOF bulk OA measurements are likely not affected by soluble inorganic matrices typical of Central Europe (i.e., internal mixtures with NH_4NO_3 and $(NH_4)_2SO_4$ concentrations up to ~10 μg m^{-3}), although effects on individual ions cannot be ruled out.

3.4. Water vapor dependence

Atmospheric water vapor concentrations are high in absolute terms and highly variable, and as a result affect the response of instruments based on chemical ionization (Vlasenko et al., 2010; Lee et al., 2014; Iyer et al., 2016; Zhao et al., 2017). Water can potentially decrease sensitivity by competing with the analyte for Na^+ ions (e.g. by displacing the analyte), or increase sensitivity by absorbing energy from Na^+-adducts, thereby stabilizing them. We therefore investigated the water vapor-dependent response of the α-pinene ozonolysis SOA mass spectrum. For these tests, SOA was generated at constant concentration in a flow tube and programmatically diluted by a dry and a wet flow. The wet flow was humidified by passing through a water bubbler held at room temperature (~25 °C). The total dilution was kept constant, but the ratio of the wet and dry flows was systematically varied to obtain relative humidities ranging from 0 to 80%. Assuming a sample flow of 0.8 L min^{-1} and 1 to 10 μL min^{-1} flow through the electrospray capillary, the working

solution provides 7 to 42 % of the total water at 50 % RH. Water vapor has a significant memory effect in the denuder used in the EESI-TOF for removing semi-volatile gases from the sample flow, therefore despite step changes in the dilution relative humidity the water vapor seen by the instrument changes much more smoothly. As a surrogate for water vapor concentration, we monitor a sodium iodide adduct generated in the spray and determine the ratio of its water-clustered and water-free forms, i.e. $[NaI(H_2O)]Na^+$ / $[NaI]Na^+$. Note that the particulate water content is insignificant compared to the ESI droplets and sample flow water vapor, and thus does not perturb either the $[NaI(H_2O)]Na^+$ / $[NaI]Na^+$ ratio or the EESI-TOF sensitivity.

The left axis of Fig. 7a (black dots) shows an example of the $[C_{10}H_{16}O_7]Na^+$ ion as a function of the $NaI(H_2O)Na^+$ / $NaINa^+$ ratio. For this ion, the instrument response is constant independent of water vapor concentration, i.e. the ratio of the ion signal (I) at a given RH to the ion signal at 0% RH ($I/I_{RH=0}$) is ~1. On the right axis (red line and shading), we show the median, 10th, and 90th percentiles for $I/I_{RH=0}$ across all detected ions as a function of $[NaI(H_2O)]Na^+$ / $[NaI]Na^+$; $I/I_{RH=0}$ = 1 is shown as a dashed green line for reference. Probability distributions of $I/I_{RH=0}$ at $[NaI(H_2O)]Na^+$ / $[NaI]Na^+$ = 0.1, 0.5, and 0.9 (with the latter condition corresponding to ~80% RH) are shown in Fig. 7b. As water vapor increases, the $I/I_{RH=0}$ distribution broadens, and the median signal decreases slightly (~15% lower at 80% RH). Note that the broadening takes place on the low-sensitivity side of the $I/I_{RH=0}$ distribution; Fig. 7b shows that many ions have a humidity-independent response, similar to $[C_{10}H_{16}O_7]Na^+$. Even for ions with the most extreme humidity dependence, at the highest water vapor concentrations measured for 90% of ions $I/I_{RH=0} > 0.60$ and for 99% $I/I_{RH=0} > 0.45$. This weak perturbation by ambient water vapor simplifies spectral interpretation, and suggests that ion chemistry occurs predominantly in the droplet phase.

3.5. Effect of particle size

Particle size can in theory affect detection in the EESI-TOF system via two mechanisms. First, particle losses may occur within the denuder by diffusion or impaction, affecting small and large particles, respectively. Second, larger particles may be incompletely extracted in the spray. These two possibilities are investigated separately. Figure 8a shows the denuder transmission efficiency as a function of particle size, as measured by a scanning mobility particle sizer (SMPS). For this test, the denuder is removed from the EESI inlet and placed within a segment of straight tubing.

SMPS measurements before and after the denuder are compared to determine transmission efficiency. The figure shows that particles are transmitted with better than 80% efficiency over the measured size range of 20 to 750 nm.

The size dependent response of the EESI extraction/ionization processes was characterized using pure dipentaerythritol particles nebulized from an aqueous solution. The polydisperse particles were dried and quantified using an SMPS system that sampled in parallel with the EESI-TOF. The size of the nebulized particles was controlled by changing the nebulizer flowrate and solution concentration. Figure 8b shows the measured sensitivity of the EESI-TOF to dipentaerythritol ($C_{10}H_{22}O_7$) as a function of the (polydisperse) particle volume distribution geometric mean diameter, which ranges between approximately 50 and 250 nm. The same sensitivity is measured independent of particle diameter, indicating complete extraction into the droplet phase and a lack of any size-dependent ionization due to solvation kinetics or incomplete extraction. Previous investigations of this effect in EESI-based aerosol systems have yielded conflicting results; our results are consistent with those of Gallimore and Kalberer (Gallimore and Kalberer, 2013), who observed no size dependence for single component OA particles with diameters ≤200 nm. For ambient aerosol, we observe a linear relationship with mass for particles of up to ~500 nm diameter (with larger sizes not yet investigated) for both methanol:water and acetonitrile:water working fluids (Qi et al., 2019; Stefenelli et al., 2019). In contrast, Kumbhani et al. (Kumbhani et al., 2018) observed incomplete extraction of $NaNO_3$ particles coated with glutaric acid, also using 1:1 methanol:water as the working fluid. One possibility is that the characteristics of the generated electrospray are significantly different in the EESI-TOF, e.g. larger droplet diameter ~~(the inner diameter of the EESI-TOF electrospray capillary is 5 times larger)~~, increased droplet number density, and/or longer droplet/analyte contact time.

We expect that the electrospray droplets are on the order of 4 to 40 µm, significantly larger than the sampled aerosol (Smith et al., 2002; Wortmann et al., 2007; Soleilhac et al., 2015; Liigand et al., 2017). In principle, as particles grow to larger diameters the aerosol particle diameter could begin to approach the diameter of the electrospray droplets. In such a limit, the extraction process would become less efficient, as particles may bounce or incompletely dissolve in the electrospray droplet plume (Wang et al., 2012). The electrospray liquid flow rate controls the electrospray droplet size distribution; therefore it is important to ensure that the flow rate is sufficiently high to keep the electrospray droplet diameter much larger than the particles to be analyzed. Low

electrospray flow rates increase instrument sensitivity by up to a factor of two (a similar trend is frequently observed for conventional ESI), but decrease response time and can introduce a size-dependent extraction efficiency at larger particle sizes. We hypothesize that these effects are due to slower flushing of the electrospray tip and surrounding areas, as well as a shift of the primary electrospray droplets towards a smaller size distribution, affecting charge density. In addition, we performed some preliminary experiments during the development of the EESI-TOF using drawn electrospray tips to generate the primary EESI droplets. Although drawn tips are known to be very efficient at generating ions in conventional electrospray sources, we found that with 15-30 μm drawn capillary tips (New Objective, Inc., Woburn, MA, USA) aerosol extraction was not efficient despite higher total primary spray ion currents, presumably due to the electrospray droplet size distribution being much smaller than our standard electrospray capillary.

4. Proof of concept measurements and applications

To assess the versatility and robustness of the EESI-TOF, proof-of-concept measurements were conducted across several laboratory and field-based platforms. Here we present sample results from the measurement of SOA generated from α-pinene ozonolysis in an environmental chamber, ground-based ambient measurements, and a proof-of-concept deployment aboard a research aircraft. The EESI-TOF performed successfully in each of these environments, demonstrating its potential for a wide range of measurement applications.

4.1. Laboratory chambers

Dark ozonolysis of α-pinene was investigated using the 27 m^3 PSI environmental chamber (Paulsen et al., 2005). Briefly, the chamber was filled with 40 to 50 ppb of ozone at 40 % RH, after which 30 ppb of α-pinene was injected and the ensuing reaction proceeded undisturbed under dark conditions for approximately 16 hours. The EESI-TOF monitored the composition of SOA particles with 1 s time resolution. A detailed analysis of the chemical composition and evolution of SOA from the α-pinene ozonolysis system as determined by the EESI-TOF is provided elsewhere, and only proof-of-concept sample data is shown here (Pospisilova et al., submitted). The time series of the summed signal of all $[C_xH_yO_z]Na^+$ ions recorded by the EESI-TOF and the measured SMPS mass are shown in Fig. 9a, with these two values compared as a scatterplot in

Fig. 9b. A strong linear correlation between the EESI-TOF and SMPS signal is observed throughout the experiment.

Figures 9c and 9d show an averaged EESI-TOF mass spectrum collected from the period of maximum suspended aerosol mass. The raw (background-subtracted) spectrum is shown in Fig. 9c. To aid the eye, $[(NaI)_n]Na^+$ clusters are removed; this is done because although the background-subtracted ~~of~~ $[(NaI)_n]Na^+$ is close to zero, ~~but~~ it ~~as~~ is the difference of two high-intensity signals and therefore remains large relative to most ions in the mass spectrum. Distinct regions are clearly visible for monomers, dimers, and higher-order oligomeric species. The dimer region is shown (on a linear axis) in the inset. Figure 9d summarizes the chemical composition in terms of a mass defect plot (difference between ion exact mass and the nearest integer, as a function of integer mass) for ions having between 7 and 10 ~~carbons~~carbon atoms. The ions are colored by carbon number and the points are sized by the signal intensity. This highlights the detailed chemical information provided by the EESI-TOF, as well providing an example of the compositional trends running throughout the spectrum.

4.2. Ambient ground-based measurements

The EESI-TOF was deployed at an urban site in Zurich, Switzerland for approximately 3 weeks during summer 2016. Stable operation was achieved for >85% of the sampling period. The EESI-TOF mass spectral time series were used to identify sources and processes governing OA in Zurich, both by direct inspection of chemical signatures and using the positive matrix factorization source apportionment technique (Stefenelli et al., 2019). Figure 10 shows the EESI-TOF mass spectrum averaged over the entire campaign, colored to highlight specific ions and families. In dark blue, we show again the set of the $[C_{7\text{-}10}H_xO_y]Na^+$ ions observed in α-pinene SOA in the PSI environmental chamber (see Fig. 9d). These ions are among the strongest contributors to the ambient OA signal during this campaign. These ions are not necessarily unique to α-pinene ozonolysis, as many can also be generated as reaction products of other terpenes and/or different oxidants (e.g. OH, NO_3 radicals). A subset of these ions may also derive from ring-opening oxidation products of aromatics. However, in a general sense, they highlight the strong contribution of biogenic emissions to summer OA in Zurich, consistent with previous studies (Daellenbach et al., 2017).

Several other species of note are highlighted in Fig. 10. The single most intense peak in the spectrum ($[C_6H_{10}O_5]Na^+$, *m/z* 185.042) is attributed to levoglucosan and its isomers. The high intensity occurs because of the significant contribution of levoglucosan to OA from biomass combustion, as well as the high sensitivity of the EESI-TOF to small saccharides (see Fig. 4). Another high intensity ion is attributed to nicotine ($[C_{10}H_{14}N_2]H^+$, *m/z* 163.123), which as a reduced nitrogen species ionizes by hydrogen abstraction rather than Na^+ adduct formation. This introduces considerable uncertainty into both the sensitivity and linearity of the EESI-TOF response to nicotine. However, the AMS nicotine tracer $C_5H_{10}N^+$ (Struckmeier et al., 2016) exhibits a strong linear correlation with the EESI-TOF nicotine measurement, suggesting that no significant non-linearities are present under the conditions encountered in Zurich (Qi et al., 2019). Finally, the spectrum shows a significant contribution from $[C_xH_yO_zN_{1-2}]Na^+$ ions, which are mostly assigned to organonitrates as discussed in detail elsewhere (Stefenelli et al., 2019).

Estimated detection limits (30 s) are shown on an ion-by-ion basis in Fig. 10b, using the same color scheme as in Fig. 10a. Detection limits are calculated as the 3-σ variation of the ion signal during the filter blank periods flanking a direct sampling interval, and the campaign median is shown. Detection limits are converted to mass assuming a uniform sensitivity of 1450 Hz / (μg m^{-3}), which corresponds to the estimated sensitivity of SOA during this campaign (Stefenelli et al., submitted). This is a rough estimate which neglects ion-dependent sensitivities and differences in molecular weight. The results are summarized in histogram form in Fig. 10c. Most species have detection limits in the range 1 to 10 ng m^{-3} (median 5.4 ng m^{-3}), with nitrogen-containing ions having slightly lower detection limits than other species. We note that these measurements utilized a methanol:H_2O working solution, and detection limits from the cleaner acetonitrile:H_2O system will likely be lower.

4.3. Aircraft deployment

Mobile sampling platforms, such as aircraft and ground vehicles, require highly time-resolved measurements. As discussed above, current OA measurements used in mobile measurements require a tradeoff between ~~extensive~~ thermal decomposition (extensive for the AMS, minor for FIGAERO-CIMS), ionization-induced fragmentation (AMS, CHARON-PTRMS), or time resolution (FIGAERO-CIMS). The EESI-TOF thus addresses an important gap in mobile aerosol

instrumentation. As a proof of concept, the EESI-TOF was deployed aboard the NOAA C-130 aircraft during the Airborne Research Instrumentation Testing Opportunity (ARISTO) 2016 test flight campaign from August 1 to 19, 2016. For these flights, the EESI inlet was installed on an API-TOF previously configured for research flights by the University of Washington (Lee et al., 2018) and operated on a pressure-controlled sampling line. In general, good performance and stability were achieved. The main difficulty encountered was icing on the sampling inlet outside the aircraft, which reduced the line pressure and flow and thereby altered the ESI spray.

Figure 11a shows a time series of $[C_6H_{10}O_5]Na^+$, which corresponds to levoglucosan and its isomers. Also shown are $[C_{10}H_{16}O_4]Na^+$ and $[C_{10}H_{16}O_5]Na^+$, which are major products of SOA formed from monoterpene oxidation. EESI-TOF data were collected at 1 Hz; each point in the figure corresponds to a 20 s re-average. At approximately 17:35, the aircraft intersects a wildfire plume. A dramatic increase in $[C_6H_{10}O_5]Na^+$ is observed, compared to only minor changes in the $[C_{10}H_{16}O_x]Na^+$ ions. The high time resolution of the EESI-TOF is critical for accurate characterization of this plume, as the entire period of intersection lasts only ~3 min. Figure 11b shows a 20 s average mass spectrum, corresponding to the period of maximum $[C_6H_{10}O_5]Na^+$ concentration. The spectrum is normalized to levoglucosan, which is the most intense peak. However, even for such a short averaging interval, many other ions are evident throughout the mass spectrum, indicating the wealth of chemical information accessible even for highly time-resolved and/or mobile measurements.

5. Conclusions

We present an extractive electrospray ionization (EESI) source coupled to TOF-MS for laboratory and field measurement of OA on a near-molecular level. The EESI-TOF achieves detection limits compatible with operation at ambient aerosol concentrations, making it the first instrument capable of real-world OA measurements without thermal decomposition, ionization-induced fragmentation, competitive ionization pathways, or separated collection/analysis stages. We observe an instrument response that is linear with mass and without a detectable dependence on the composition of the OA matrix for a dipentaerythritol/α-pinene SOA test system. Ambient measurements also suggest that bulk OA detection is not significantly affected by a changing matrix of soluble inorganic compounds. Changing water vapor concentrations only slightly affect

the instrument response to most ions, with a ~50% decrease in sensitivity observed for the most extreme cases. Particle transmission to the EESI source is greater than 80% between 20 and 750 nm, with particles of at least 250 nm (and likely 500 nm) completely extracted in the spray (larger particles remain to be tested). The EESI-TOF was successfully deployed for environmental chamber experiments, ground-based ambient sampling, and tests flights aboard a research aircraft, highlighting its versatility and range of potential applications.

The EESI-TOF sensitivity to SOA generated from a ~~range~~ set of individual precursor gases varies within a factor of ~~6~~ 15~~for most precursors~~. Larger variations in sensitivity were found between pure organic standards. However, compound-by-compound sensitivities in laboratory-generated SOA are proportional to those determined by the collisionally-limited FIGAERO-I-CIMS within ±50%. This shows promise for an eventual parameterization of the EESI-TOF sensitivity to unknown species, and further suggests that the EESI-TOF responds in a similar way to collision-limited CIMS approaches and that the mass spectra thus approximately reflect the actual distribution of detectable compounds.

The working fluid and ionization scheme plays an important role in both instrument stability/performance and the set of detectable compounds. Here we have focused on positive ion detection using a 1:1 methanol:water system (with a subset of data using 1:1 acetonitrile:water), with 100 ppm NaI added to suppress all ionization pathways except for Na^+-adduct formation. This controlled ionization is highly desirable, and contributes to the system linearity, lack of matrix effects, and spectral interpretation. These Na^+-based systems allow detection of most compounds comprising atmospheric OA, with the notable exceptions of non-oxygenated species and organosulfates. However, different extraction/ionization schemes could be envisaged for different chemical targets, increasing the overall utility of the EESI-TOF.

Acknowledgements

This work was supported by the Swiss National Science Foundation (starting grant BSSGI0_155846). The ARISTO test flight program is funded by the U.S. National Science Foundation Deployment Pool. We thank Tofwerk AG and the PSI machine shop for supporting the construction and integration of the EESI source. We also thank David Bell, Deepika Bhattu, and Yandong Tong (PSI) for useful discussions on acetonitrile clustering, H_2O working fluid, and

large particle detection. Rene Richter and Christoph Hueglin are gratefully acknowledged for logistical support of the Zurich deployment.

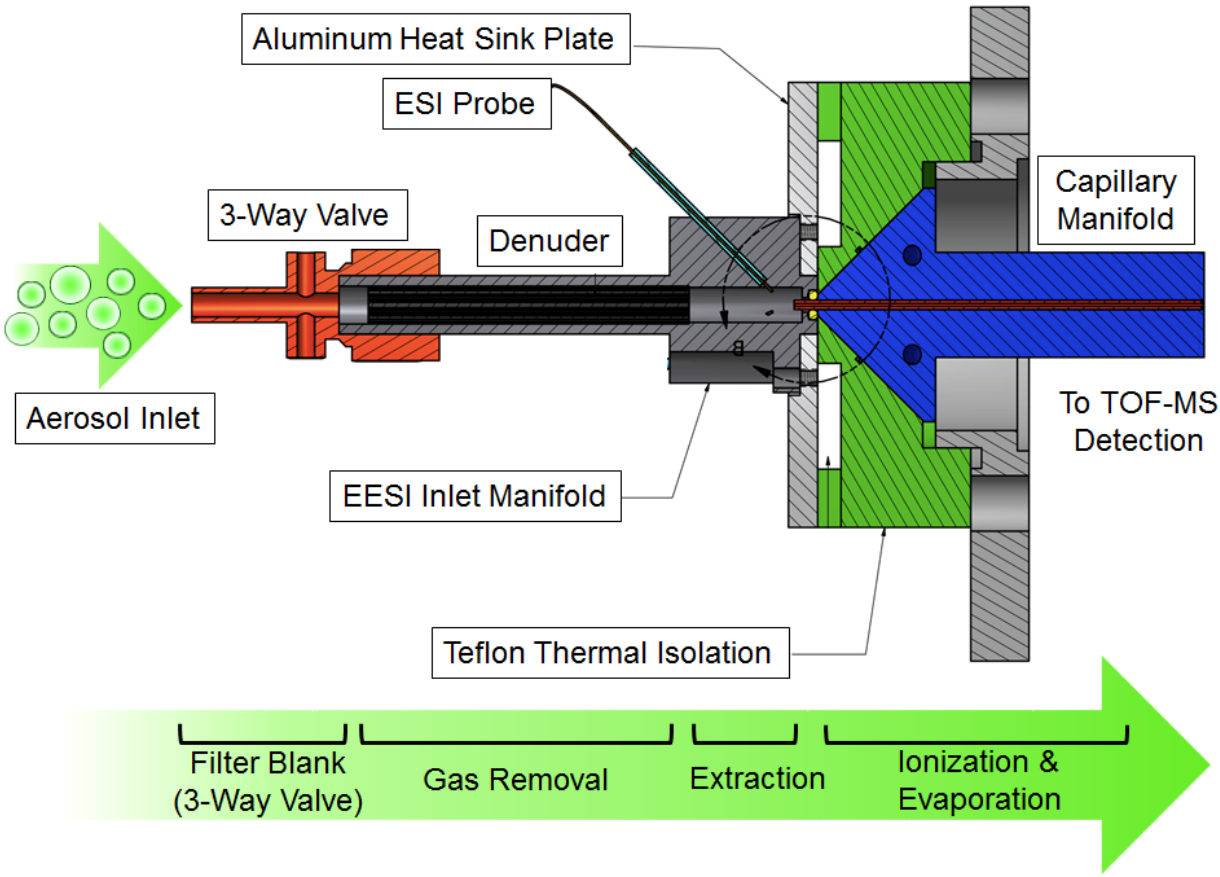

Figure 1. Schematic of the EESI-TOF inlet and ion source, including connection to TOF-MS.

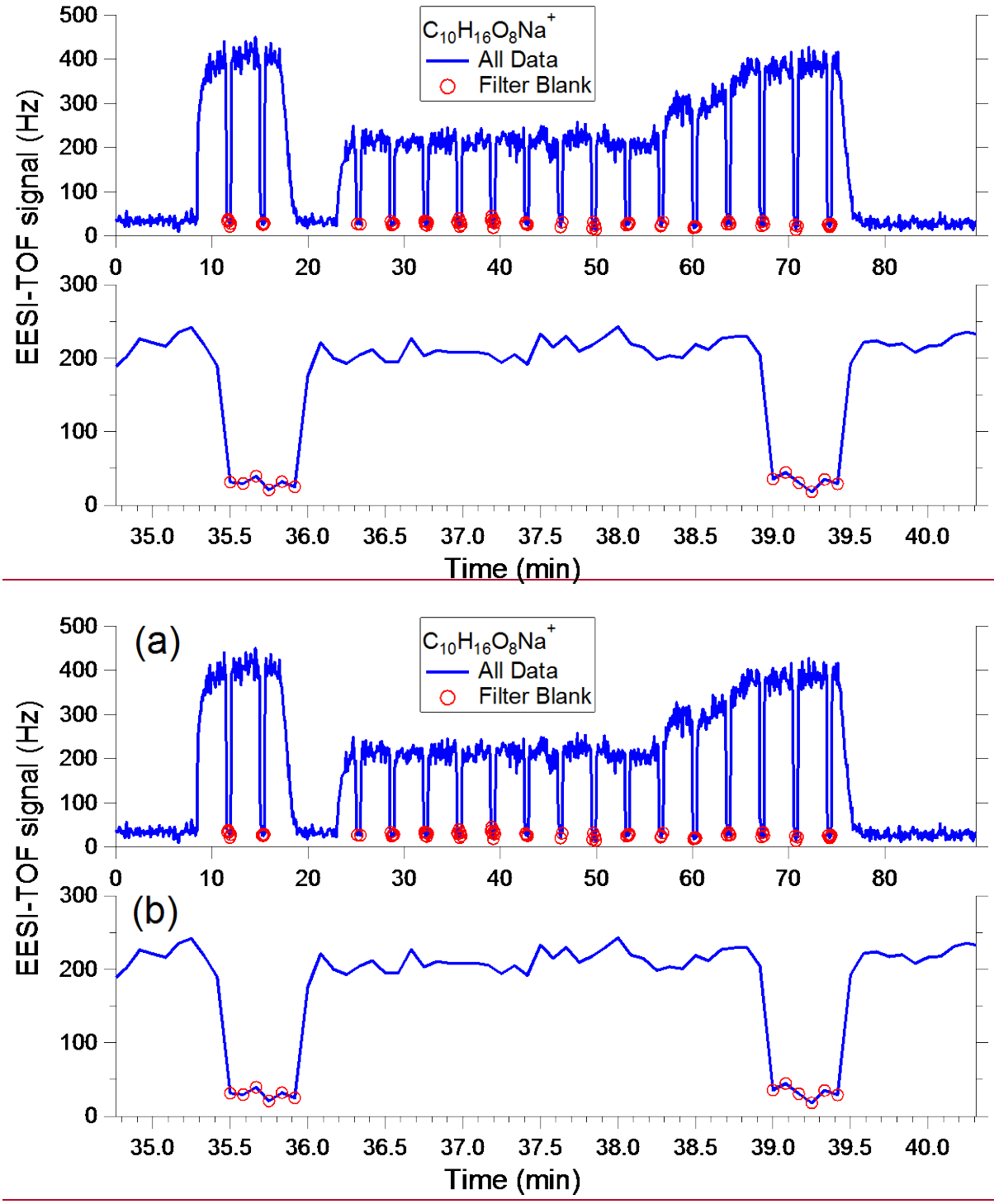

Figure 2. (a) Sample time series of $[C_{10}H_{16}O_8]Na^+$ measured in SOA generated from α-pinene ozonolysis, showing aerosol measurement periods (3 min) interspersed with filter blanks (30 s). The difference between these two conditions yields the signal due to sampled particles. (b)

Expanded view of two measurement/filter cycles showing; instrument response to filter switching is ~5 s.

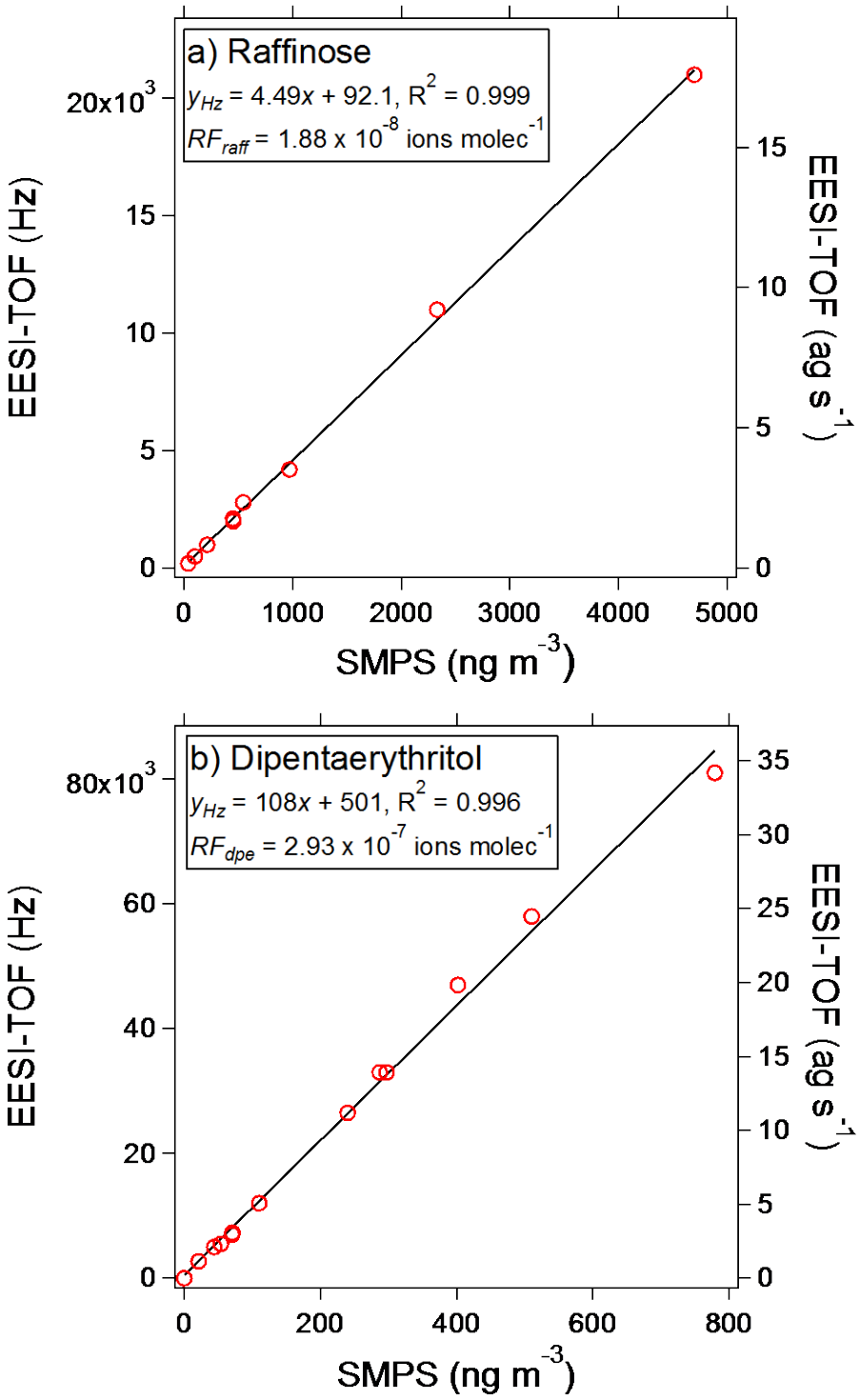

Figure 3. EESI-TOF signal as a function of mass concentration measured by an SMPS, assuming spherical particles with the material density of the pure compound, for raffinose (a) and dipentaerythritol (b). The EESI-TOF signal is represented both in terms of the flux of ions (left axis) and mass (right axis) reaching the detector.

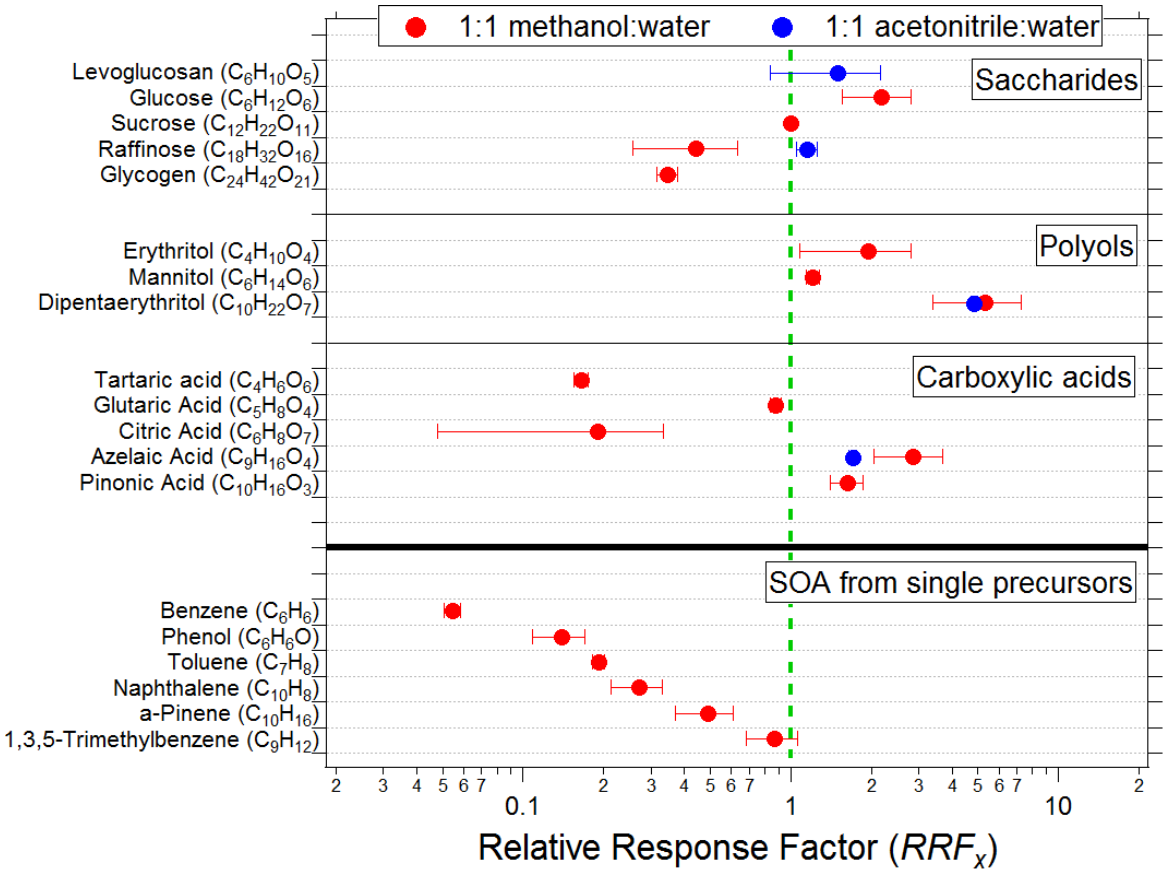

Figure 4. EESI-TOF sensitivity (ions molecule^{-1}, see Eq. 1) relative to that of sucrose for pure components and SOA formed by OH-initiated oxidation of single precursors in a PAM flow reactor. Red points denote a 1:1 methanol:water working fluid; blue denotes 1:1 acetonitrile:water. All configurations use 100 ppm NaI as a dopant, and all ions are detected as $[M]Na^+$.

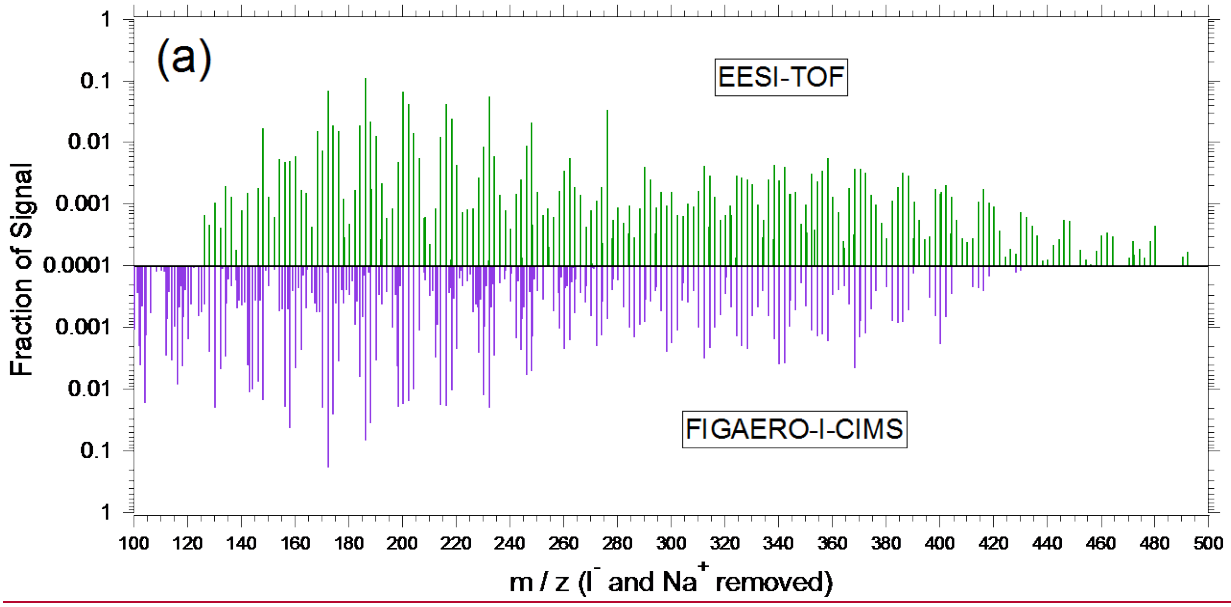
(a)
EESI-TOF
FIGAERO-I-CIMS
Fraction of Signal
1
0.1
0.01
0.001
0.0001
0.001
0.01
0.1
1
100 120 140 160 180 200 220 240 260 280 300 320 340 360 380 400 420 440 460 480 500
m / z (I⁻ and Na⁺ removed)

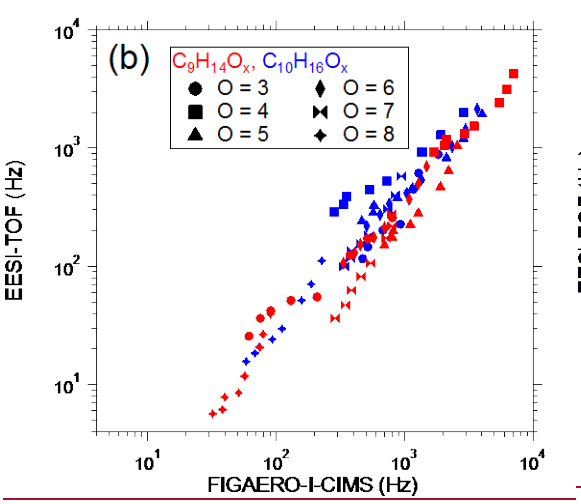
(b)
C9H14Ox, C10H16Ox
O = 3
O = 4
O = 5
O = 6
O = 7
O = 8
EESI-TOF (Hz)
FIGAERO-I-CIMS (Hz)

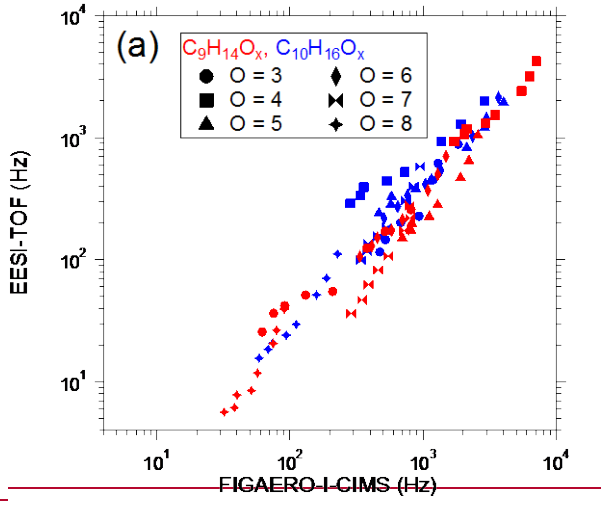
(a)
C9H14Ox, C10H16Ox
O = 3
O = 4
O = 5
O = 6
O = 7
O = 8
EESI-TOF (Hz)
FIGAERO-I-CIMS (Hz)

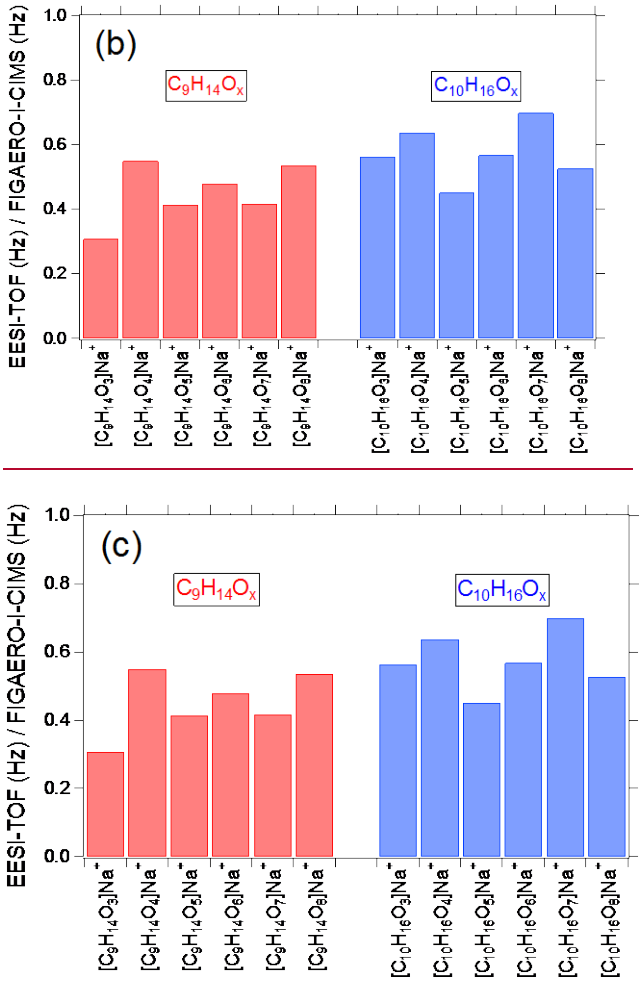

Figure 5. (a) Particle-phase mass spectra of SOA from α-pinene ozonolysis measured by the EESI-TOF (top, green) and FIGAERO-I-CIMS (purple, bottom). Spectra are normalized such that the sum across the displayed *m/z* window is 1, and the reported *m/z* are after subtraction of Na^+ (EESI-TOF) and I^- (FIGAERO). (~~a~~b) EESI-TOF signal (Hz) as a function of FIGAERO-I-CIMS (Hz) for the $[C_9H_{14}O_x]Na^+$ (red) and $[C_{10}H_{16}O_x]Na^+$ (blue) ion series. Marker shape denotes number of oxygen atoms. (~~b~~c) Slopes of linear fits to individual ions for the $[C_9H_{14}O_x]Na^+$ (red) and $[C_{10}H_{16}O_x]Na^+$ (blue) ion series. All fits are conducted using orthogonal distance regression with unconstrained intercepts.

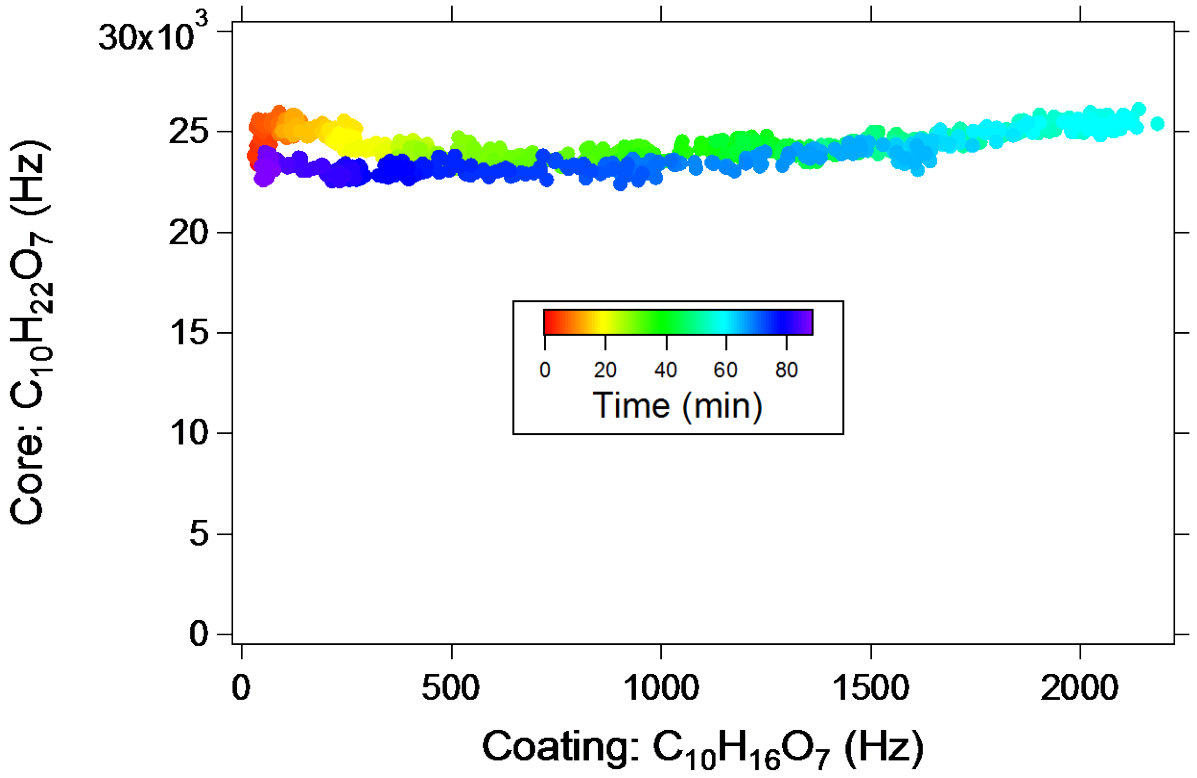

Figure 6. Dipentaerythritol $[C_{10}H_{22}O_7]Na^+$ signal measured in a flow tube as a function of $[C_{10}H_{H16}O_7]Na^+$ signal, which is proportional to condensed SOA mass. The maximum $[C_{10}H_{H16}O_7]Na^+$ signal corresponds to approximately 75 μg m^{-3} of SOA, of which approximately 40% occurs as a coating on the dipentaerythritol seed, increasing the particle diameter from 20 to 70 nm. Points are colored by time, showing an increase and then decrease of coating material.

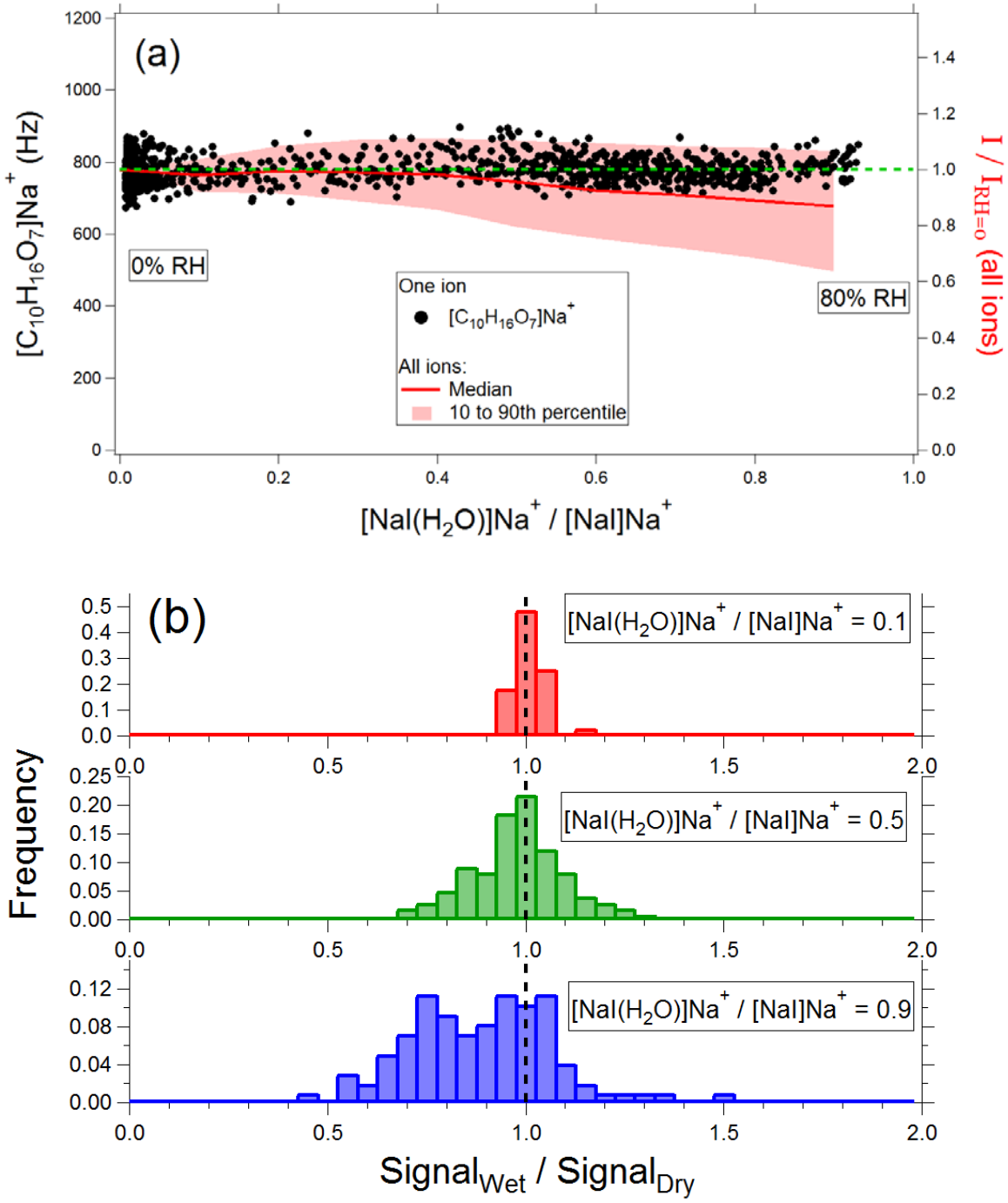

Figure 7. Effect of water vapor on EESI-TOF response. (a) Left axis, black points: $[C_{10}H_{16}O_7]Na^+$ signal as a function of $[NaI](H_2O)]Na^+$ / $[NaI]Na^+$. Right axis, red shading: median, 10th, and 90th percentiles of $I/I_{RH=0}$ for all measured ions. (b) Probability distributions of $I/I_{RH=0}$ at $[NaI](H_2O)]Na^+$ / $[NaI]Na^+$ = 0.1, 0.5, and 0.9, where $[NaI](H_2O)]Na^+$ / $[NaI]Na^+$ = 0.9 corresponds to 80% RH.

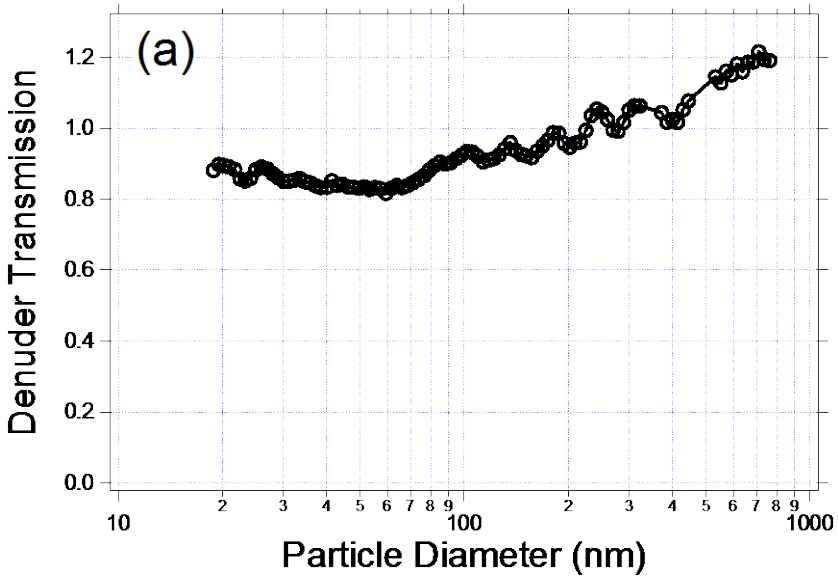
(a)
Denuder Transmission
1.2
1.0
0.8
0.6
0.4
0.2
0.0
10
2
3
4
5
6
7
8
9
100
2
3
4
5
6
7
8
9
1000
Particle Diameter (nm)

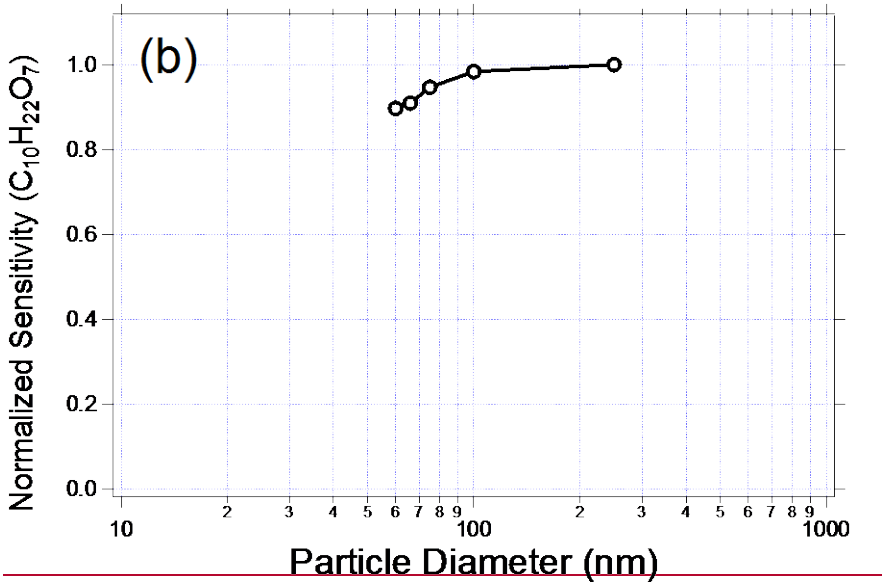

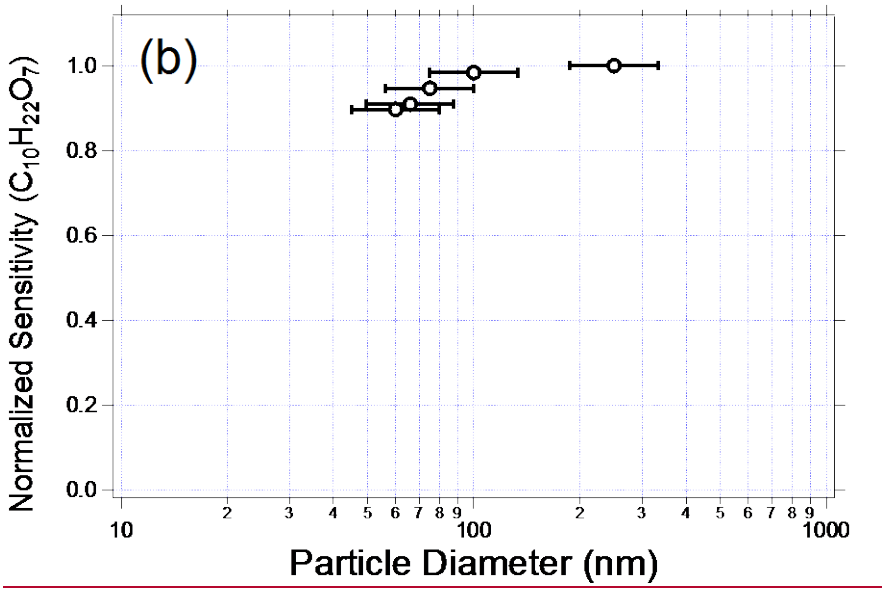

Figure 8. (a) Particle transmission through the denuder as a function of diameter. (b) Measured sensitivity of dipentaerythritol as a function of particle diameter. Error bars denote the mobility diameters corresponding to the half-maxima of the polydisperse particle volume distribution.

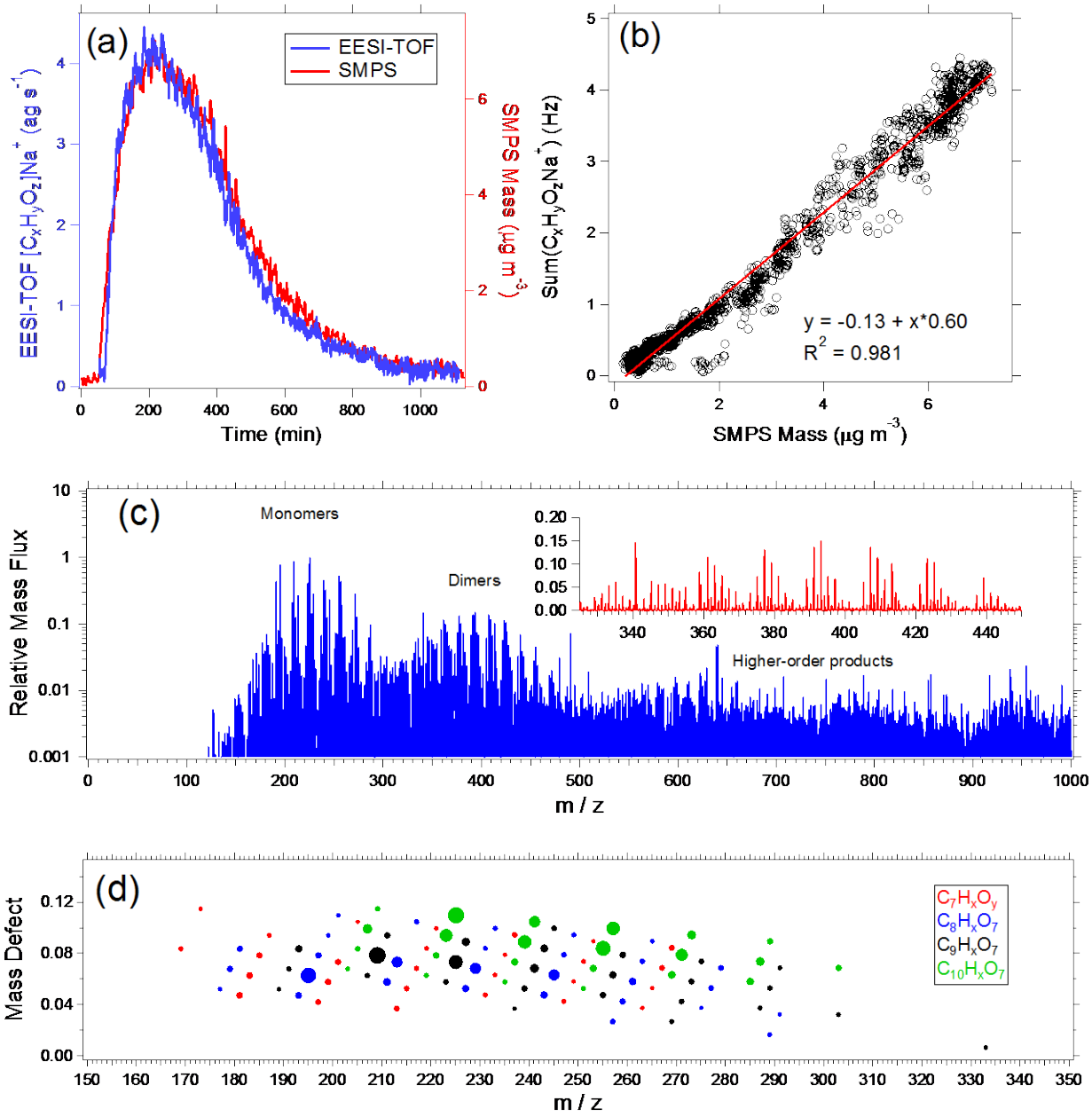

Figure 9. Sample EESI-TOF data from α-pinene ozonolysis in an environmental chamber. (a) Summed signal from all $[C_xH_yO_z]Na^+$ ions measured by the EESI-TOF and particle mass measured by the SMPS (effective density = 1.2 g cm^{-3}) as a function of time after beginning of reaction. (b) EESI-TOF $[C_xH_yO_z]Na^+$ signal as a function of SMPS mass. (c) Averaged EESI-TOF mass spectrum, with dimer region expanded on linear scale in inset. (d) Mass defect plot of monomer region, with markers sized by signal intensity and colored by number of carbon atoms.

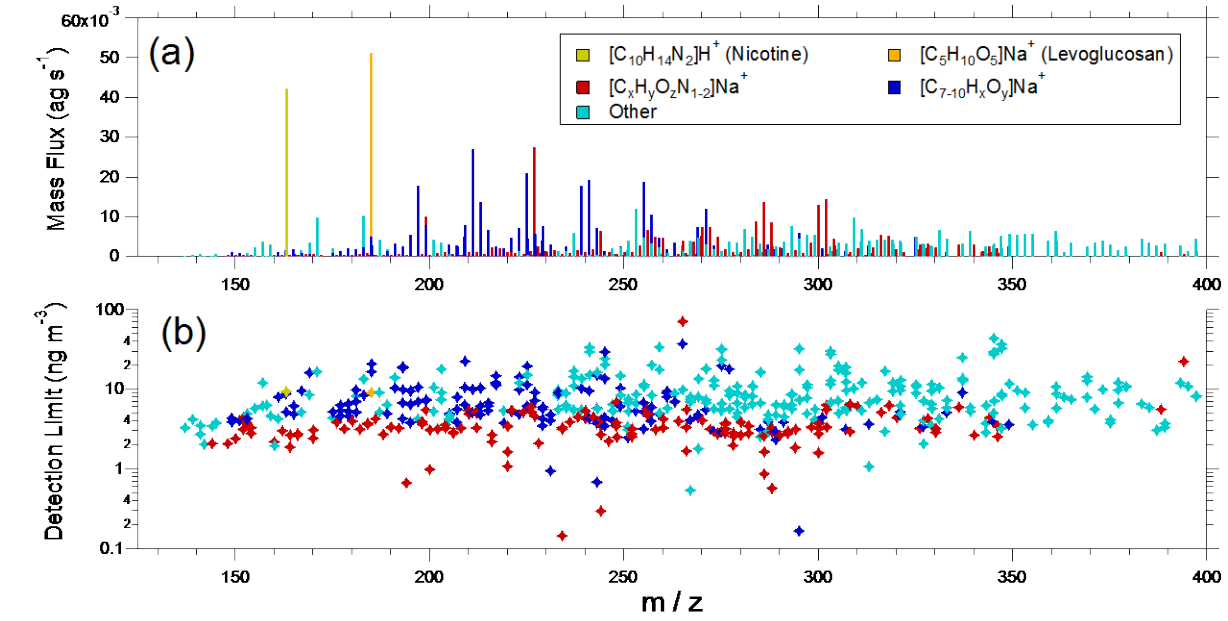
(a)
Mass Flux (ag s-1)
60x10-3
[C10H14N2]H+ (Nicotine)
[C5H10O5]Na+ (Levoglucosan)
[CxHyOzN1-2]Na+
[C7-10HxOy]Na+
Other
(b)
Detection Limit (ng m-3)
m / z

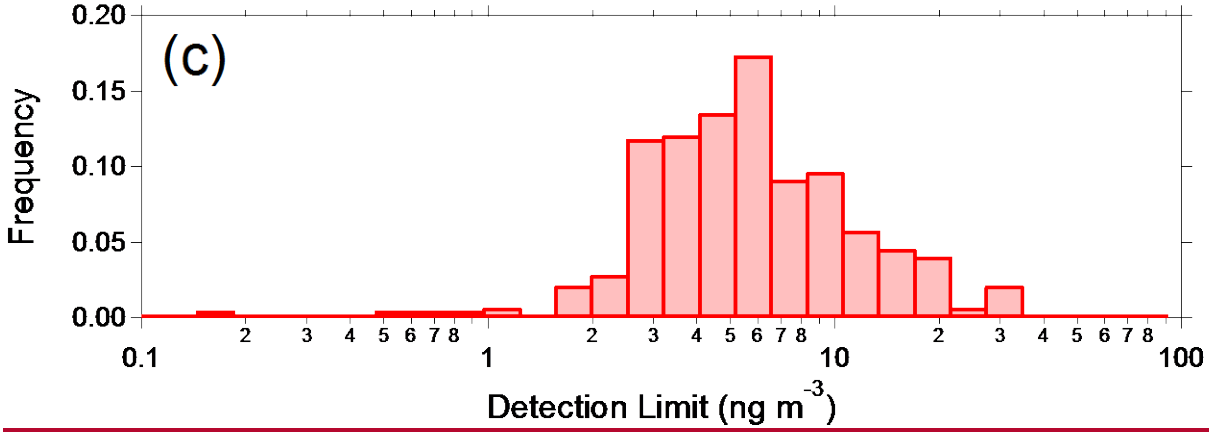
(c)
Frequency
Detection Limit (ng m-3)

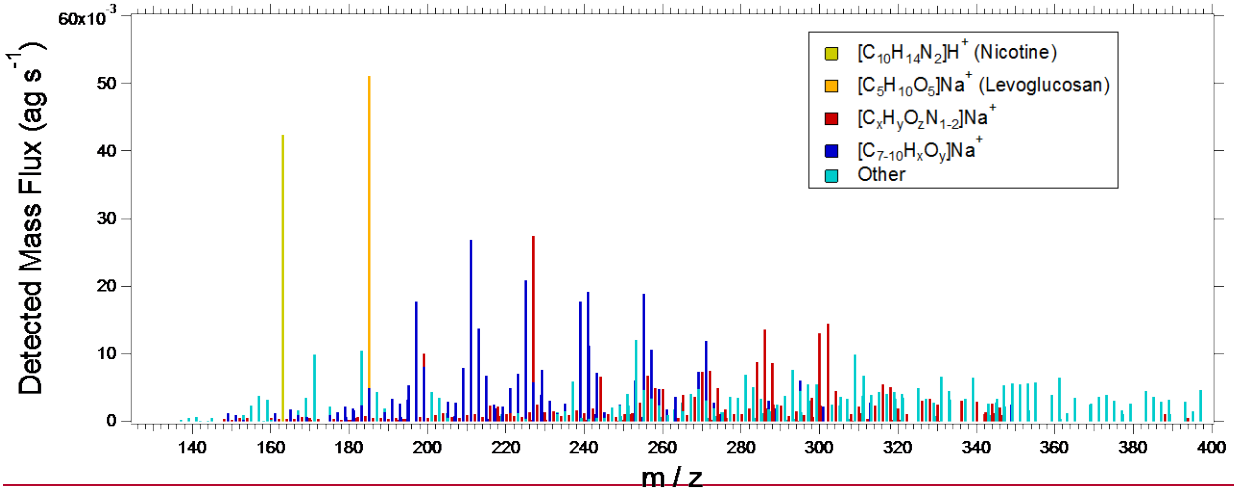
Detected Mass Flux (ag s-1)
60x10-3
[C10H14N2]H+ (Nicotine)
[C5H10O5]Na+ (Levoglucosan)
[CxHyOzN1-2]Na+
[C7-10HxOy]Na+
Other
m / z

Figure 10. (a) Campaign average EESI-TOF mass spectrum from summer measurements in Zurich, Switzerland. Selected ions and families are colored as shown in the legend. Note the x-axis begins at *m/z* 125 due to blanking of smaller ions by the quadrupole ion guides. (b) Campaign median detection limits (30 s), colored as in Fig. 10a. Detection limits are calculated as 3-σ variation of the filter blank periods flanking a direct sampling interval, and assuming a uniform sensitivity of 1450 Hz / (µg m^{-3}). (c) Probability distribution of campaign median detection limits.

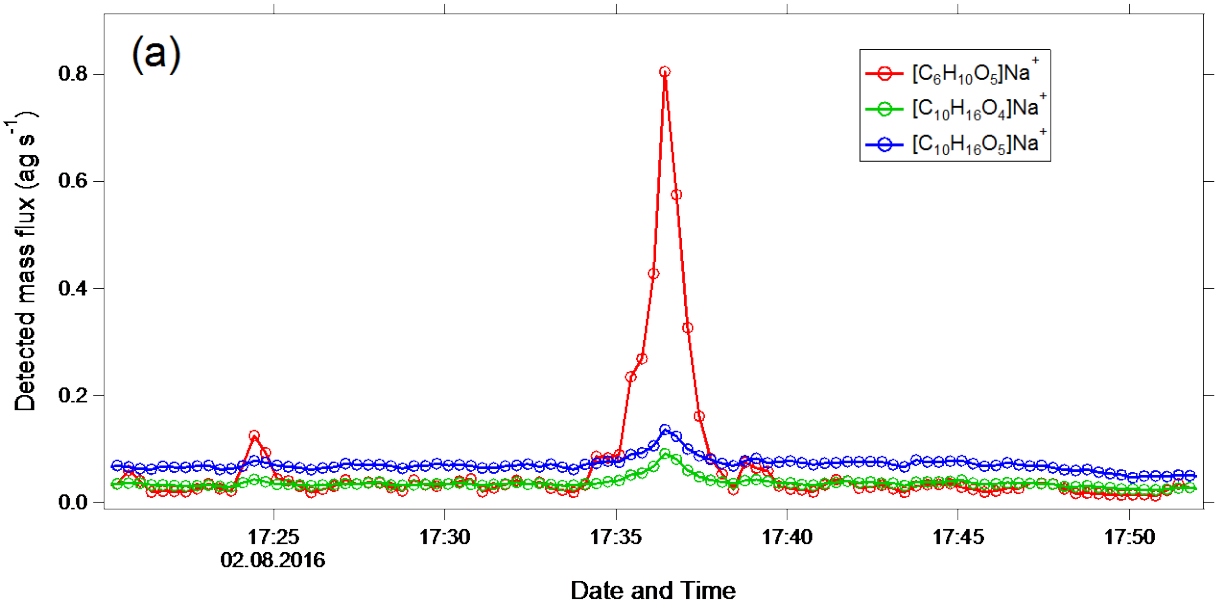

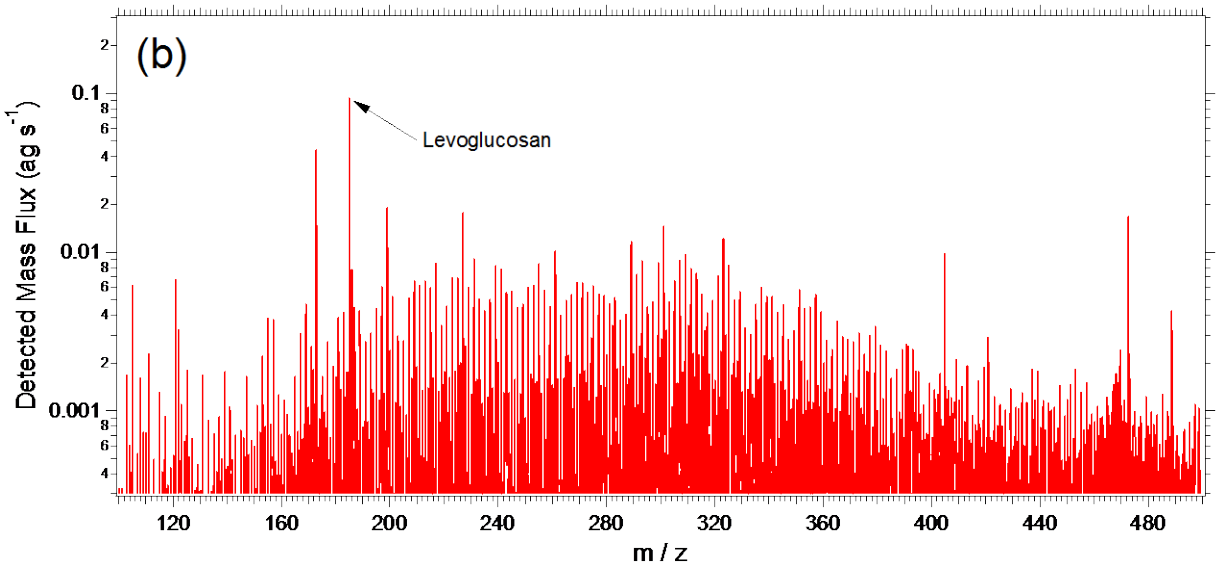

Figure 11. (a) Time series of selected ions showing transect of a wildfire plume. Shown are $[C_6H_{10}O_5]Na^+$ (levoglucosan and its isomers) and the monoterpene SOA-influenced ions $[C_{10}H_{16}O_4]Na^+$ and $[C_{10}H_{16}O_5]Na^+$. (b) Mass spectrum (20 s average) during the peak of the wildfire plume with levoglucosan labelled.

References

Bertrand, A., Yuan, B., Stefenelli, G., Qi, L., Pospisilova, V., Tong, Y., Sepideh, E., Huang, R.-J., El Haddad, I., Slowik, J. G., and Prevot, A. S. H.: Characterization of fresh and aged solid fuel combustion organic aerosol by extractive electrospray ionization time-of-flight mass spectrometer (EESI-TOF), Environ. Sci. Technol., submitted.

Brüggemann, M., Karu, E., Stelzer, T., and Hoffmann, T.: Real-time analysis of ambient organic aerosols using aerosol flowing atmospheric-pressure afterglow mass spectrometry (AeroFAPA-MS), Environ. Sci. Technol., 49, 5571-5578, 10.1021/es506186c, 2015.

Brüggemann, M., Poulain, L., Held, A., Stelzer, T., Zuth, C., Richters, S., Mutzel, A., van Pinxteren, D., Iinuma, Y., Katkevica, S., Rabe, R., Herrmann, H., and Hoffmann, T.: Real-time detection of highly oxidized organosulfates and BSOA marker compounds during the F-BEACh 2014 field study, Atmos. Chem. Phys., 17, 1453-1469, 10.5194/acp-17-1453-2017, 2017.

Canagaratna, M. R., Jayne, J. T., Jimenez, J. L., Allan, J. D., Alfarra, M. R., Zhang, Q., Onasch, T. B., Drewnick, F., Coe, H., Middlebrook, A., Delia, A., Williams, L. R., Trimborn, A. M., Northway, M. J., DeCarlo, P. F., Kolb, C. E., Davidovits, P., and Worsnop, D. R.: Chemical and microphysical characterization of ambient aerosols with the Aerodyne aerosol mass spectrometer, Mass Spec. Rev., 26, 185-222, 10.1002/mas.20115, 2007.

Cappiello, A., Famiglini, G., Palma, P., Pierini, E., Termopoli, V., and Trufelli.: Overcoming matrix effects in liquid chromatograph-mass spectrometry, Anal. Chem., 80, 9343-9348, 10.1021/ac801312, 2008.

Chen, H., Venter, A., and Cooks, R. G.: Extractive electrospray ionization for direct analysis of undiluted urine, milk and other complex mixtures without sample preparation, Chem. Commun., 19, 2042-2044, 10.1039/b602614a, 2006.

Chen, H., Gamez, G., and Zenobi, R.: What can we learn from ambient ionization techniques?, J. Am. Soc. Mass Spec., 20, 1947-1963, 2009.

Daellenbach, K. R., Stefenelli, G., Bozzetti, C., Vlachou, A., Fermo, P., Gonzalez, R., Piazzalunga, A., Colombi, C., Canonaco, F., Hueglin, C., Kaspar-Giebl, A., Jaffrezo, J.-L., Bianchi, F., Slowik, J. G., Baltensperger, U., El Haddad, I., and Prévôt, A. S. H.: Long-term chemical analysis and organic aerosol source apportionment at nine sites in Central Europe: source identification and uncertainty assessment, Atmos. Chem. Phys., 17, 13265-13282, 10.5194/acp-17-13265-2017, 2017.

Doezema, L. A., Longin, T., Cody, W., Perraud, V., Dawson, M. L., Ezell, M. J., Greaves, J., Johnson, K. R., and Finlayson-Pitts, B. J.: Analysis of secondary organic aerosols in air using extractive electrospray ionization mass spectrometry (EESI-MS), RSC Advances, 2, 2930-2938, 10.1039/C2RA00961G, 2012.

Eichler, P., Müller, M., D'Anna, B., and Wisthaler, A.: A novel inlet system for online chemical analysis of semi-volatile submicron particulate matter, Atmos. Meas. Tech., 8, 1353-1360, 10.5194/amt-8-1353-2015, 2015.

Furey, A., Moriarty, M., Bane, V., Kinsella, B., and Lehane, M.: Ion suppression; a critical review on causes, evaluation, prevention, and applications, Talanta, 115, 104-122, 10.1016/j.talanta.2013.03.048, 2013.

Gallimore, P. J., and Kalberer, M.: Characterizing an extractive electrospray ionization (EESI) source for the online mass spectrometry analysis of organic aerosols, Environ. Sci. Technol., 47, 7324-7331, 10.1021/es305199h, 2013.

Gallimore, P. J., Giorio, C., Mahon, B. M., and Kalberer, M.: Online molecular characterisation of organic aerosols in an atmospheric chamber using extractive electrospray ionisation mass spectrometry, Atmos. Chem. Phys., 17, 14485-14500, 10.5194/acp-17-14485-2017, 2017.

Gard, E., Mayer, J. E., Morrical, B. D., Dienes, T., Fergenson, D. P., and Prather, K. A.: Real-time analysis of individual atmospheric aerosol particles: design and performance of a portable ATOFMS, Anal. Chem., 69, 4083-4091, 10.1021/ac970540n, 1997.

Goldstein, A. H., and Galbally, I. E.: Known and unexplored organic constituents in the earth's atmosphere, Environ. Sci. Technol., 41, 1514-1521, Doi 10.1021/Es072476p, 2007.

Gu, H. W., Chen, H. W., Pan, Z. Z., Jackson, A. U., Talaty, N., Xi, B. W., Kissinger, C., Duda, C., Mann, D., Raftery, D., and Cooks, R. G.: Monitoring diet effects via biofluids and their implications for metabolomics studies, Anal. Chem., 79, 89-97, 10.1021/ac060946c, 2007.

Hallquist, M., Wenger, J. C., Baltensperger, U., Rudich, Y., Simpson, D., Claeys, M., Dommen, J., Donahue, N. M., George, C., Goldstein, A. H., Hamilton, J. F., Herrmann, H., Hoffmann, T., Iinuma, Y., Jang, M., Jenkin, M. E., Jimenez, J. L., Kiendler-Scharr, A., Maenhaut, W., McFiggans, G., Mentel, T. F., Monod, A., Prevot, A. S. H., Seinfeld, J. H., Surratt, J. D., Szmigielski, R., and Wildt, J.: The formation, properties and impact of secondary organic aerosol: current and emerging issues, Atmos. Chem. Phys., 9, 5155-5236, 2009.

Holzinger, R., Williams, J., Herrmann, F., Lelieveld, J., Donahue, N. M., and Röckmann, T.: Aerosol analysis using a Thermal-Desorption Proton-Transfer-Reaction Mass Spectrometer (TD-PTR-MS): a new approach to study processing of organic aerosols, Atmos. Chem. Phys., 10, 2257-2267, 10.5194/acp-10-2257-2010, 2010.

Horan, A. J., Gao, Y., Hall, W. A., and Johnston, M. V.: Online characterization of particles and gases with an ambient electrospray ionization source, Anal. Chem., 84, 9253-9258, 10.1021/ac302024y, 2012.

Isaacman, G., Kreisberg, N. M., Yee, L. D., Worton, D. R., Chan, A. W. H., Moss, J. A., Hering, S. V., and Goldstein, A. H.: Online derivatization for hourly measurements of gas- and particle-phase semi-volatile oxygenated organic compounds by thermal desorption aerosol gas chromatography (SV-TAG), Atmos. Meas. Tech., 7, 4417-4429, 10.5194/amt-7-4417-2014, 2014.

Iyer, S., Lopez-Hilfiker, F. D., Lee, B. H., Thornton, J. A., and Kurtén, T.: Modeling the detection of organic and inorganic compounds using iodide-based chemical ionization, J. Phys. Chem. A, 120, 576-587, 2016.

Jimenez, J. L., Canagaratna, M. R., Donahue, N. M., Prevot, A. S., Zhang, Q., Kroll, J. H., DeCarlo, P. F., Allan, J. D., Coe, H., Ng, N. L., Aiken, A. C., Docherty, K. S., Ulbrich, I. M., Grieshop, A. P., Robinson, A. L., Duplissy, J., Smith, J. D., Wilson, K. R., Lanz, V. A., Hueglin, C., Sun, Y. L., Tian, J., Laaksonen, A., Raatikainen, T., Rautiainen, J., Vaattovaara, P., Ehn, M., Kulmala, M., Tomlinson, J. M., Collins, D. R., Cubison, M. J., Dunlea, E. J., Huffman, J. A., Onasch, T. B., Alfarra, M. R., Williams, P. I., Bower, K., Kondo, Y., Schneider, J., Drewnick, F., Borrmann, S., Weimer, S., Demerjian, K., Salcedo, D., Cottrell, L., Griffin, R., Takami, A., Miyoshi, T., Hatakeyama, S., Shimono, A., Sun, J. Y., Zhang, Y. M., Dzepina, K., Kimmel, J. R., Sueper, D., Jayne, J. T., Herndon, S. C., Trimborn, A. M., Williams, L. R., Wood, E. C., Middlebrook, A. M., Kolb, C. E., Baltensperger, U., and Worsnop, D. R.: Evolution of organic aerosols in the atmosphere, Science, 326, 1525-1529, 10.1126/science.1180353, 2009.

Junninen, H., Ehn, M., Petäjä, T., Luosujärvi, L., Kotiaho, T., Kostiainen, R., Rohner, U., Gonin, M., Fuhrer, K., Kulmala, M., and Worsnop, D. R.: A high-resolution mass spectrometer to measure atmospheric ion composition, Atmos. Meas. Tech., 3, 1039-1053, 10.5194/amt-3-1039-2010, 2010.

Kebarle, P., and Peschke, M.: On the mechanisms by which the charged droplets produced by electrospray lead to gas phase ions, Anal. Chim. Act., 406, 11-35, 10.1016/s0003-2670(99)00598-x, 2000.

Kristensen, K., Bilde, M., Aalto, P. P., Petaja, T., and Glasius, M.: Denuder/filter sampling of organic acids and organosulfates at urban and boreal forest sites: gas/particle distribution and possible sampling artifacts, Atmos. Environ., 130, 36-53, 10.1016/j.atmosenv.2015.10.046, 2016.

Kroll, J. H., Donahue, N. M., Jimenez, J. L., Kessler, S. H., Canagaratna, M. R., Wilson, K. R., Altieri, K. E., Mazzoleni, L. R., Wozniak, A. S., Bluhm, H., Mysak, E. R., Smith, J. D., Kolb, C. E., and Worsnop, D. R.: Carbon oxidation state as a metric for describing the chemistry of atmospheric organic aerosol, Nature Chemistry, 3, 133-139, 10.1038/NCHEM.948, 2011.

Kumbhani, S., Longin, T., Wingen, L. M., Kidd, C., Perraud, V., and Finlayson-Pitts, B. J.: New mechanism of extractive electrospray ionization mass spectrometry for heterogeneous solid particles, Anal. Chem., 90, 2055-2062, 10.1021/acs.analchem.7b04164, 2018.

Lambe, A. T., Ahern, A. T., Williams, L. R., Slowik, J. G., Wong, J. P. S., Abbatt, J. P. D., Brune, W. H., Ng, N. L., Wright, J. P., Croasdale, D. R., Worsnop, D. R., Davidovits, P., and Onasch, T. B.: Characterization of aerosol photooxidation flow reactors: heterogeneous oxidation, secondary organic aerosol formation and cloud condensation nuclei activity measurements, Atmos. Meas. Tech., 4, 445-461, 10.5194/amt-4-445-2011, 2011.

Laskin, J., Laskin, A., Roach, P. J., Slysz, G. W., Anderson, G. A., Nizkorodov, S. A., Bones, D. L., and Nguyen, L. Q.: High-resolution desorption electrospray ionization mass spectrometry for chemical characterization of organic aerosols, Anal. Chem., 82, 2048-2058, 10.1021/ac902801f, 2010.

Lee, B. H., Lopez-Hilfiker, F. D., Mohr, C., Kurtén, T., Worsnop, D. R., and Thornton, J. A.: An iodide-adduct high-resolution time-of-flight chemical-ionization mass spectrometer: application to atmospheric inorganic and organic compounds, Environ. Sci. Technol., 48, 6309-6317, 2014.

Lee, B. H., Lopez-Hilfiker, F. D., Veres, P. R., McDuffie, E. E., Fibiger, D. L., Sparks, T. L., Ebben, C. J., Green, J. R., Schroder, J. C., Campuzano-Jost, P., Iyer, S., D'Ambro, E. L., Schobesberger, S., Brown, S. S., Wooldridge, P. J., Cohen, R. C., Fiddler, M. N., Bililign, S., Jimenez, J. L., Kurtén, T., Weinheimer, A. J., Jaegle, L., and Thornton, J. A.: Flight deployment of a high-resolution time-of-flight chemical ionization mass spectrometer: observations of reactive halogen and nitrogen oxide species, J. Geophys. Res. - Atmos., 123, 7670-7686, 10.1029/2017JD028082, 2018.

Liigand, P., Heering, A., Kaupmees, K., Leito, I., Girod, M., Antoine, R., and Kruve, A.: The evolution of electrospray generated droplets is not affected by ionization mode, J. Am. Soc. Mass Spec., 28, 2124-2131, 10.1007/s13361-017-1737-5, 2017.

Lopez-Hilfiker, F. D., Mohr, C., Ehn, M., Rubach, F., Kleist, E., Wildt, J., Mentel, T. F., Lutz, A., Hallquist, M., Worsnop, D., and Thornton, J. A.: A novel method for online analysis of gas and particle composition: description and evaluation of a Filter Inlet for Gases and AEROsols (FIGAERO), Atmos. Meas. Tech., 7, 983-1001, 10.5194/amt-7-983-2014, 2014.

Lopez-Hilfiker, F. D., Mohr, C., Ehn, M., Rubach, F., Kleist, E., Wildt, J., Mentel, T. F., Carrasquillo, A. J., Daumit, K. E., Hunter, J. F., Kroll, J. H., Worsnop, D. R., and Thornton, J. A.: Phase partitioning and volatility of secondary organic aerosol components formed from α-pinene ozonolysis and OH oxidation: the importance of accretion products and other low volatility compounds, Atmos. Chem. Phys., 15, 7765-7776, 10.5194/acp-15-7765-2015, 2015.

Lopez-Hilfiker, F. D., Iyer, S., Mohr, C., Lee, B. H., D'Ambro, E. L., Kurtén, T., and Thornton, J. A.: Constraining the sensitivity of iodide adduct chemical ionization mass spectrometry to multifunctional organic molecules using the collision limit and thermodynamic stability of iodide ion adducts, Atmos. Meas. Tech., 9, 1505-1512, 10.5194/amt-9-1505-2016, 2016.

Molteni, U., Bianchi, F., Klein, F., El Haddad, I., Frege, C., Rossi, M. J., Dommen, J., and Baltensperger, U.: Formation of highly oxygenated organic molecules from aromatic compounds, Atmos. Chem. Phys., 18, 1909-1921, 10.5194/acp-18-1909-2018, 2018.

Müller, M., Eichler, P., D'Anna, B., Tan, W., and Wisthaler, A.: Direct sampling and analysis of atmospheric particulate organic matter by proton-transfer-reaction mass spectrometry, Anal. Chem., 89, 10889-10897, 10.1021/acs.analchem.7b02582, 2017.

Murphy, D. M., Cziczo, D. J., Froyd, K. D., Hudson, P. K., Matthew, B. M., Middlebrook, A. M., Peltier, R. E., Sullivan, A., Thomson, D. S., and Weber, R. J.: Single-particle mass spectrometry of tropospheric aerosol particles, J. Geophys. Res. - Atmos., 111, 10.1029/2006jd007340, 2006.

Paulsen, D., Dommen, J., Kalberer, M., Prévôt, A. S. H., Richter, R., Sax, M., Steinbacher, M., Weingartner, E., and Baltensperger, U.: Secondary organic aerosol formation by irradiation of

1,3,5-trimethylbenzene-NO_x-H_2O in a new reaction chamber for environmental chemistry and physics, Environ. Sci. Technol., 39, 2668-2678, 2005.

Pejov, L.: Metal cations: a density functional, coupled cluser, and quadratic configuration interaction study, International Journal of Quantum Chemistry, 86, 356-367, 10.1002/qua.10022, 2002.

Pospisilova, V., Lopez-Hilfiker, F. D., Bell, D., El Haddad, I., Mohr, C., Huang, W., Heikkinen, L., Xiao, M., Dommen, J., Prévôt, A. S. H., Baltensperger, U., and Slowik, J. G.: On the fate of oxygenated organic molecules in atmospheric aerosol particles, Science Advances, submitted.

Qi, L., Chen, M.-D., Stefenelli, G., Pospisilova, V., Tong, Y.-D., Bertrand, A., Hueglin, C., Rigler, M., Ge, X.-L., Baltensperger, U., Prévôt, A. S. H., and Slowik, J. G.: Real-time source quantification of wintertime secondary organic aerosol in Zurich using an extractive electrospray ionization time-of-flight mass spectrometer (EESI-TOF), Atmos. Chem. Phys., 19, 8037-8062, 10.5194/acp-19-8037-2019, 2019.

Reemstsma, T., These, A., Venkatachari, P., Xia, X. Y., Hopke, P. K., Springer, A., and Linscheid, M.: Identification of fulvic acids and sulfated and nitrated analogues in atmospheric aerosol by electrospray ionization Fourier transform ion cyclotron resonance mass spectrometry, Anal. Chem., 78, 8299-8304, 2006.

Roach, P. J., Laskin, J., and Laskin, A.: Nanospray desorption electrospray ionization: an ambient method for liquid-extraction surface sampling in mass spectrometry, Analyst, 135, 2233-2236, 10.1039/c0an00312c, 2010.

Rodgers, M. T., and Armentrout, P. B.: Absolute binding energies of sodium ions to short chain alcohols, $C_nH_{2n+2}O$, n = 1-4, determined by threshold collision-induced dissociation experiments and ab initio theory, J. Phys. Chem. A, 103, 4955-4963, 10.1021/jp990656i, 1999.

Smith, J. N., Flagan, R. C., and Beauchamp, J. L.: Droplet evaporation and discharge dynamics in electrospray ionization, J. Phys. Chem. A, 106, 9957-9967, 10.1021/jp025723e, 2002.

Soleilhac, A., Dagany, X., Dugourd, P., Girod, M., and Antoine, R.: Correlating droplet size with temperature changes in electrospray source by optical methods, Anal. Chem., 87, 8210-8217, 10.1021/acs.analchem.5b00976, 2015.

Stefenelli, G., Lopez-Hilfiker, F. D., Pospisilova, V., Vogel, A., Hüglin, C., Baltensperger, U., Prévôt, A. S. H., and Slowik, J. G.: Source apportionment of ambient organic aerosol by online extractive electrospray ionization time-of-flight mass spectrometry (EESI-TOF), Atmos. Chem. Phys. Discuss., 10.5194/acp-2019-361, 2019.

Stefenelli, G., Lopez-Hilfiker, F. D., Pospisilova, V., Vogel, A., Hüglin, C., Baltensperger, U., Prévôt, A. S. H., and Slowik, J. G.: Source apportionment of ambient organic aerosol by online extractive electrospray ionization time-of-flight mass spectrometry (EESI-TOF), Atmospheric Chemistry and Physics Discussions, submitted.

Struckmeier, C., Drewnick, F., Fachinger, F., Gobbi, G. P., and Borrmann, S.: Atmospheric aerosols in Rome, Italy: sources, dynamics and spatial variations during two seasons, Atmos. Chem. Phys., 16, 15277-15299, 10.5194/acp-16-15277-2016, 2016.

Stüber, M., and Reemtsma, T.: Evaluation of three calibraiton methods to compensate matrix effects in environmental analysis with LC-ESI-MS, Analytial and Bioanalytical Chemistry, 378, 910-916, 10.1007/s00216-003-2442-8, 2004.

Subramanian, R., Khlystov, A. Y., Cabada, J. C., and Robinson, A. L.: Positive and negative artifacts in particulate organic carbon measurements with denuded and undenuded sampler configurations, Aerosol Sci. Technol., 38, 27-48, 10.1080/02786820390229354, 2004.

Surratt, J. D., Gomez-Gonzalez, Y., Chan, A. W., Vermeylen, R., Shahgholi, M., Kleindienst, T. E., Edney, E. O., Offenberg, J. H., Lewandowski, M., Jaoui, M., Maenhaut, W., Claeys, M., Flagan, R. C., and Seinfeld, J. H.: Organosulfate formation in biogenic secondary organic aerosol, J. Phys. Chem. A, 112, 8345-8378, 10.1021/jp802310p, 2008.

Timkovsky, J., Chan, A. W. H., Dorst, T., Goldstein, A. H., Oyama, B., and Holzinger, R.: Comparison of advanced offline and in situ techniques of organic aerosol composition measurement during the CalNex campaign, Atmos. Meas. Tech., 8, 5177-5187, 10.5194/amt-8-5177-2015, 2015.

Turpin, B. J., Huntzicker, J. J., and Hering, S. V.: Investigation of organic aerosol sampling artifacts in the Los Angeles basin, Atmos. Environ., 28, 3061-3071, 10.1016/1352-2310{94)00133-6, 1994.

Vlasenko, A., Macdonald, A. M., Sjostedt, S. J., and Abbatt, J. P. D.: Formaldehyde measurements by proton transfer reaction - mass spectrometry (PTR-MS): correction for humidity effects, Atmos. Meas. Tech., 3, 1055-1062, 10.5194/amt-3-1055-2010, 2010.

Volkamer, R., Jimenez, J. L., San Martini, F., Dzepina, K., Zhang, Q., Salcedo, D., Molina, L. T., Worsnop, D. R., and Molina, M. J.: Secondary organic aerosol formation from anthropogenic air pollution: rapid and higher than expected, Geophys. Res. Lett., 33, L17811, 2006.

Wang, R., Groehn, A. J., Zhu, L., Dietiker, R., Wegner, K., Guenther, D., and Zenobi, R.: On the mechanism of extractive electrospray ionization (EESI) in the dual-spray configuration, Anal. Bioanal. Chem., 402, 2633-2643, 10.1007/s00216-011-5471-8, 2012.

Wortmann, A., Kistler-Momotova, A., Zenobi, R., Heine, M. C., and Wilhelm, O. P., S. E.: Shrinking droplets in electrospray ionization and their influence on chemical equilibria, J. Am. Soc. Mass Spec., 18, 385-393, 10.1016/j.jasms.2006.10.010, 2007.

Zelenyuk, A., and Imre, D.: Single particle laser ablation time-of-flight mass spectrometer: an introduction to SPLAT, Aerosol Sci. Technol., 39, 554-568, 10.1080/027868291009242, 2005.

Zhang, H., Surratt, J. D., Lin, Y.-H., Bapat, J., and Kamens, R. M.: Effect of relative humidity on SOA formation from isoprene/NO photooxidation: enhancement of 2-methylglyceric acid and its

corresponding oligoesters under dry conditions, Atmos. Chem. Phys., 11, 6411-6424, 10.5194/acp-11-6411-2011, 2011.

Zhang, X., McVay, R. C., Huang, D. D., Dalleska, N. F., Aumont, B., Flagan, R. c., and Seinfeld, J. H.: Formation and evolution of molecular products in a-pinene secondary organic aerosol, Proc. Nat. Acad. Sci., 112, 14168-14173, 10.1073/pnas.1517742112, 2015.

Zhang, X., Dalleska, N. F., Huang, D. D., Bates, K. H., Sorooshian, A., Flagan, R. C., and Seinfeld, J. H.: Time-resolved molecular characterization of organic aerosols by PILS + UPLC/ESI-Q-TOFMS, Atmos. Environ., 130, 180-189, 10.1016/j.atmosenv.2015.08.049, 2016.

Zhao, Y., Chan, J. K., Lopez-Hilfiker, F. D., McKeown, M. A., D'Ambro, E. L., Slowik, J. G., Riffell, J. A., and Thornton, J. A.: An electrospray chemical ionization source for real-time measurement of atmospheric organic and inorganic vapors, Atmos. Meas. Tech., 10, 3609-3625, 10.5194/amt-10-3609-2017, 2017.

Zhou, Z. Q., Jin, M., Ding, J. H., Zhou, Y. M., Zheng, J., and Chen, H. W.: Rapid detection of atrazine and its metabolite in raw urine by extractive electrospray ionization mass spectrometry, Metabolomics, 3, 101-104, 10.1007/s11306-006-0050-2, 2007.